



2023 COASTAL MASTER PLAN

DETERMINING SUBSIDENCE RATES FOR USE IN PREDICTIVE MODELING

ATTACHMENT B3

REPORT: VERSION 03

DATE: MARCH 2021

PREPARED BY: CATHERINE FITZPATRICK, KRISTA L. JANKOWSKI, AND DENISE REED



COASTAL PROTECTION AND
RESTORATION AUTHORITY
150 TERRACE AVENUE
BATON ROUGE, LA 70802
WWW.COASTAL.LA.GOV

COASTAL PROTECTION AND RESTORATION AUTHORITY

This document was developed in support of the 2023 Coastal Master Plan being prepared by the Coastal Protection and Restoration Authority (CPRA). CPRA was established by the Louisiana Legislature in response to Hurricanes Katrina and Rita through Act 8 of the First Extraordinary Session of 2005. Act 8 of the First Extraordinary Session of 2005 expanded the membership, duties, and responsibilities of CPRA and charged the new authority to develop and implement a comprehensive coastal protection plan, consisting of a master plan (revised every six years) and annual plans. CPRA's mandate is to develop, implement, and enforce a comprehensive coastal protection and restoration master plan.

CITATION

Fitzpatrick, C., Jankowski, K. L., & Reed, D. (2021). 2023 Coastal Master Plan: Attachment B3: Determining Subsidence Rates for Use in Predictive Modeling. Version 3. (p. 71). Baton Rouge, Louisiana: Coastal Protection and Restoration Authority.

ACKNOWLEDGEMENTS

This document was developed as part of broader plans for model improvement in support of the 2023 Coastal Master Plan under the guidance of the Modeling Decision Team:

- Coastal Protection and Restoration Authority (CPRA) of Louisiana – Elizabeth Jarrell (formerly CPRA), Stuart Brown, Ashley Cobb, Catherine Fitzpatrick (formerly CPRA), Krista Jankowski, David Lindquist, Sam Martin, and Eric White
- University of New Orleans – Denise Reed

The following Coastal Protection and Restoration Authority (CPRA) staff provided guidance and review of this document:

- Stuart Brown
- Elizabeth Jarrell (formerly CPRA)
- Eric White
- Syed Khalil
- Leigh Anne Sharpe
- Tommy McGinnis
- Angelina Freeman
- James Pahl
- Rick Raynie
- Darin Lee

The following experts provided external review for a previous draft version of this document and their contributions were important to shaping the approach presented here:

- Mead Allison, Tulane University
- Michael Blum, University of Kansas
- Cathleen Jones, Jet Propulsion Laboratory
- Mark Kulp, University of New Orleans
- John Rybczyk, Western Washington University
- Carol Wilson, Louisiana State University

EXECUTIVE SUMMARY

To develop the 2023 Coastal Master Plan, the Louisiana Coastal Protection and Restoration Authority (CPRA) and partners are implementing updates to several predictive models developed through previous master plan efforts. The Integrated Compartment Model (ICM), Storm Surge and Waves models (ADCIRC and SWAN), and Coastal Louisiana Risk Assessment model (CLARA) are used to understand future landscape change and changing vulnerability under various future environmental scenarios. In the master plan process, one goal of modeling landscape change and storm surge-based flood risk is to explore the effects of different possible future conditions on the performance of restoration and protection projects and inform decision-making processes. A second goal is to allow for communication with coastal residents about possible future coastal conditions. Model inputs, such as the current landscape and existing hydrologic connections, provide a starting point for these predictive models. One model input that is of particular importance (due to the sensitivity of the ICM to its influence) is the rate of subsidence across coastal Louisiana. The ICM uses subsidence to lower the land surface, while additional components of the model separately account for surface sediment deposition and wetland soil development, both of which can offset the effects of subsidence on surface elevation. Subsidence is also applied in risk modeling using CLARA.

Refining subsidence rates for use as model inputs for the ICM is an important part of updating predictive models for the 2023 Coastal Master Plan. Recently published studies provide new information on subsidence rates in coastal Louisiana. These include small and large-scale observational studies, as well as data re-analyses and data syntheses. This report provides background information related to considerations of subsidence in predictive modeling, including introducing the factors that influence subsidence rates across coastal Louisiana, describing how subsidence rates were considered in the 2012 and 2017 Coastal Master Plans, and briefly summarizing recent literature available to support determination of updated subsidence rates. The report then details the approach to determine subsidence rates across Louisiana's coastal zone for use in predictive modeling for the 2023 Coastal Master Plan.

The 2023 subsidence approach relies on the development of several subsidence maps for coastal Louisiana. The first is a deep subsidence (DS) map derived from data from geodetic survey benchmarks, both primary (Continuously Operating Reference Stations or CORS) and secondary (CPRA/National Geodetic Survey (NGS) benchmarks). The resulting map shows variation in DS rates across the coast, with broad spatial patterns related to underlying geology and past depositional processes. The Chenier Plain in western Louisiana largely shows low DS rates that range from 0 to 1.5 mm/yr. Rates less than 2.5 mm/yr are also found on the North Shore of Lake Pontchartrain and areas east of New Orleans. Along the gulf coast, rates of 5-6 mm/yr are shown in the Teche-Vermilion basin. For much of the Mississippi River delta plain, DS rates range from ~4 mm/yr to ~12 mm/yr. Higher DS rates occur in the lower basins that are underlain by some of the thickest Holocene sediment packages, with rates up to 14.8 mm/yr throughout lower Terrebonne Basin, and up to 7 mm/yr in

lower Barataria Basin and parts of outer Pontchartrain and Breton Sound Basin. The highest DS rates of up to 16.8 mm/yr occur in the Bird's Foot Delta.

In addition, two shallow subsidence (SS) maps were created using data derived from the most up-to-date rod surface elevation table-marker horizon (RSET-MH) measurements taken at Coastwide Reference Monitoring System (CRMS) sites. CRMS-derived SS rates were aggregated by ICM ecoregions (i.e., at a sub-regional scale). For each ICM ecoregion, first quartile and median SS values were calculated. Two maps were created due to variability in the SS data and these will be applied separately for two environmental scenarios in the master plan analysis. Ecoregion SS values using first quartile values range from negative values (-0.6 mm/yr) in Sabine to 5.8 mm/yr in southeast Barataria. When median values are used, SS rates range from 1.0 mm/yr in the Calcasieu ecoregion to 7.3 mm/yr in the Bird's Foot Delta. As the SS maps are derived from CRMS data, no SS rates are calculated for the Atchafalaya Basin and the Verret Basin.

Total subsidence (TS) rates (i.e., the sum of SS and DS) are determined by creating composite maps. As there are two SS maps, two maps for TS result – one representing a lower total subsidence rate scenario and the other a higher subsidence rate scenario. These maps can be combined with other information (e.g., sea level rise rates), in environmental scenarios used to drive future conditions for model simulations. In general, the highest rates of total subsidence are in the Bird's Foot Delta (> 18 mm/yr in both lower and higher scenarios) with slightly lower rates in central Terrebonne and near the Atchafalaya and Wax Lake Deltas (8-16 mm/yr). Lowest rates are in the western Chenier Plain and the North Shore of Lake Pontchartrain, <4 mm/yr and <6 mm/yr for the lower and higher scenarios respectively). This report discusses the expert panel-based approach used in the 2012 and 2017 Coastal Master Plans and the details of the approach used for the 2023 Coastal Master Plan, including the assumptions and limitations of the 2023 approach and the consistency of derived rates with recent studies.

TABLE OF CONTENTS

COASTAL PROTECTION AND RESTORATION AUTHORITY	2
CITATION	2
ACKNOWLEDGEMENTS	3
EXECUTIVE SUMMARY	4
TABLE OF CONTENTS	6
LIST OF TABLES	8
LIST OF FIGURES	8
LIST OF ABBREVIATIONS	10
1.0 INTRODUCTION	11
1.1 Purpose of Defining Subsidence Rates for Use in the 2023 Coastal Master Plan	11
1.2 Subsidence in Coastal Louisiana: Contributing Processes and Measurement Approaches	12
2.0 PREVIOUS MASTER PLANS	16
2.1 Subsidence in the 2012 Coastal Master Plan	16
2.2 Subsidence in the 2017 Coastal Master Plan	18
3.0 NEW INFORMATION ON SUBSIDENCE RATES SINCE THE 2017 COASTAL MASTER PLAN	19
4.0 SUBSIDENCE APPROACH FOR THE 2023 COASTAL MASTER PLAN	23
4.1 Approach	23
4.2 Assumptions and Limitations	24
5.0 DEVELOPMENT OF A DEEP SUBSIDENCE MAP FOR COASTAL LOUISIANA	27
5.1 Deep Subsidence Data	27
5.2 Determining Deep Subsidence rates	28
5.3 Spatial Application of Deep Subsidence	29
5.4 Assumptions and Limitations of Deep Subsidence Approach	31
6.0 DEVELOPMENT OF A SHALLOW SUBSIDENCE MAP FOR COASTAL LOUISIANA	33
6.1 Shallow Subsidence Data	33
6.2 Determining Shallow Subsidence Rates	33
6.3 Spatial Application of Shallow Subsidence	36
6.4 Assumptions and Limitations of Shallow Subsidence Approach	40
7.0 SUMMARY	41

7.1 Deep Subsidence Patterns41

7.2 Shallow Subsidence Patterns41

7.3 Total Subsidence Rates42

8.0 REFERENCES 46

9.0 APPENDICES 53

APPENDIX A: COMMON APPROACHES TO SUBSIDENCE MEASUREMENT 54

APPENDIX B: SUPPLEMENTAL INFORMATION FOR SUBSIDENCE MAP DEVELOPMENT
..... 57

LIST OF TABLES

Table 1. General description of processes contributing to subsidence in coastal Louisiana.	12
Table 2. Summary of information on subsidence rates from recent studies of coastal Louisiana.	20
Table 3. Plot Set Sampling Years. Ranges of years indicate the observation window for the plot set.	34
Table 4. Aggregated shallow subsidence statistics and values by ecoregion.	37
Table A1. Several approaches to measuring rates of subsidence are described.	54
Table B1. All primary and secondary benchmark stations (CORS/NGS) from Byrnes et al. (2019) and ACRE (2019), as well as supplementary data compiled by CPRA and used in the calculation of DS.	58
Table B2. Shallow subsidence rates (Figure 8), surface elevation change (Appendix B, Figure B3), and vertical accretion rates (Appendix B, Figure B4) by CRMS site. ..	62
Table B3.	69

LIST OF FIGURES

Figure 1. Temporal and spatial scales of the different processes contributing to subsidence.	14
Figure 2. Temporal and spatial scales of various subsidence measurement techniques (modified Yuill, et al., 2009).	15
Figure 3. Previously used plausible subsidence rate ranges for coastal Louisiana.	17
Figure 4. Representation of measurements used to develop subsidence rates for the 2023 Coastal Master Plan.	24
Figure 5. Potential overlap of DS and SS in meters developed through surface differencing.	26
Figure 6. Coastwide deep subsidence point data, including the source for benchmark analysis.	28
Figure 7. Deep subsidence map of coastal Louisiana.	30
Figure 8. Shallow subsidence RSET-MH point data from 203 CRMS sites.	35
Figure 9. Map of 25 ecoregions defined for the 2023 Coastal Master Plan. Ecoregions used to aggregate data for the shallow subsidence surface map.	36
Figure 10. First quartile of shallow subsidence rate point data aggregated by ecoregion across coastal Louisiana.	38
Figure 11. Median of shallow subsidence rate point data aggregated by ecoregion across coastal Louisiana.	39
Figure 12. Coastwide map of total subsidence rates for the lower scenario.	43

Figure 13. Coastwide map of total subsidence rates for the higher scenario.	44
Figure B1. Sample calculations of vertical displacement at a CORS site, in this case at the GRIS site.	57
Figure B2. Vertical accretion (top) and surface elevation (bottom) data graphed as time series data.	61
Figure B3. The distribution of surface elevation change (SEC) rates (from site establishment through fall 2019 measurement campaigns) at CRMS sites across coastal Louisiana.	70
Figure B4. The distribution of vertical accretion (VA) rates (from site establishment through fall 2019 measurement campaigns) at CRMS sites across coastal Louisiana.	71

LIST OF ABBREVIATIONS

ACRE	APPLIED COASTAL RESEARCH AND ENGINEERING
ADCIRC	ADVANCED CIRCULATION MODEL
CLARA	COASTAL LOUISIANA RISK ASSESSMENT
CORS	CONTINUOUSLY OPERATING REFERENCE STATION
CPRA	COASTAL PROTECTION AND RESTORATION AUTHORITY
CRMS	COASTWIDE REFERENCE MONITORING SYSTEM
DS	DEEP SUBSIDENCE
GIA	GLACIO-ISOSTATIC ADJUSTMENT
GPS	GLOBAL POSITIONING SYSTEM
HUC-12.....	HYDROLOGIC UNIT CODE 12
ICM	INTEGRATED COMPARTMENT MODEL
INSAR.....	INTERFEROMETRIC SYNTHETIC APERTURE RADAR
NGS	NATIONAL GEODETIC SURVEY
MH	MARKER HORIZON
RMSE.....	ROOT MEAN SQUARE ERROR
RSET	ROD SURFACE ELEVATION TABLE
SEC	SURFACE ELEVATION CHANGE
SS.....	SHALLOW SUBSIDENCE
SWAN	SIMULATING WAVES NEARSHORE MODEL
TS	TOTAL SUBSIDENCE
VA.....	VERTICAL ACCRETION

1.0 INTRODUCTION

1.1 PURPOSE OF DEFINING SUBSIDENCE RATES FOR USE IN THE 2023 COASTAL MASTER PLAN

Subsidence is the gradual or sudden lowering of the land surface over time. It has long been recognized as a key driver of coastal change in Louisiana (e.g., Gagliano et al., 2003; Roberts et al., 1994) due to the direct impact of subsidence on landscape change and its contribution to relative sea level rise rates. Predictive modeling of future coastal conditions has been undertaken by the state of Louisiana to select coastal protection and restoration projects that address changing conditions and anticipated environmental challenges. The analytical approach used in master plan development and project selection (CPRA, 2017; Peyronnin et al., 2013) allows for landscape change and storm surge-based flood risk to be responsive to changing land elevations based on predicted future environmental conditions. Landscape change predictions are developed using the ICM (White et al., 2019; White et al., 2017), which simulates long-term hydrology, wetland morphology, and vegetation and barrier shorelines and dynamics for the Louisiana coast across a variety of environmental conditions. Landscape conditions from the ICM are passed to storm surge and waves models (Cobell et al., 2013), which are used to assess the effects of coastal storms on storm surge-based flood risk and damages (Fischbach et al., 2017). The storm surge (ADCIRC), wave (SWAN), and damage (CLARA) models also consider the effectiveness of structural protection projects and risk reduction projects (i.e., elevations, floodproofing, and voluntary acquisition of structures) on expected annual damages.

Assumed rates of future subsidence are required to drive these analyses because subsidence results in an annual lowering of the modelled landscape as well as any restoration/risk reduction features (e.g., levees) superimposed on that landscape. ICM landscape change projections have been shown to be particularly sensitive to this model input (Meselhe et al., 2017b). Given the importance of subsidence to the changing landscape and future risk, the question of what rates to use to characterize subsidence across coastal Louisiana is a consequential consideration. Previous master plan efforts have considered the effects of subsidence on future environmental conditions and project outcomes, though subsidence rates used as model inputs for the ICM were based on expert judgement rather than being explicitly data-driven, which potentially contributed additional uncertainty to future outcomes.

This report describes the approach used to determine subsidence rates across coastal Louisiana to support predictive modeling for the 2023 Coastal Master Plan. The report introduces the factors (i.e., geologic and geomorphic processes) that influence subsidence rates across the coast, describes how subsidence rates were determined for the 2012 and 2017 Coastal Master Plans, and briefly summarizes recent literature on subsidence rates in coastal Louisiana. It then details the approach used to determine subsidence rates for use in predictive modeling for the 2023 Coastal Master Plan.

1.2 SUBSIDENCE IN COASTAL LOUISIANA: CONTRIBUTING PROCESSES AND MEASUREMENT APPROACHES

There is broad scientific agreement that an array of factors contribute to subsidence in coastal Louisiana. Yuill et al. (2009) provide an overview of the contributing processes and their relevance to coastal Louisiana, and these factors are also noted by more recent reviews (e.g., Frederick et al., 2019; Higgins, 2016). Table 1 provides an overview of contributing processes.

Table 1. General description of processes contributing to subsidence in coastal Louisiana (after Yuill et al., 2009).

PROCESS	GENERAL DESCRIPTION
Tectonic Subsidence	TECTONIC PROCESSES (I.E., PROCESSES RELATING TO THE STRUCTURE AND EVOLUTION OF THE LITHOSPHERE) INCLUDING NATURAL FAULT PROCESSES SUCH AS GULF OF MEXICO BASIN DEVELOPMENT, SHELF-EDGE GROWTH FAULTING, AND SALT MOVEMENT (I.E., HALOKINESIS).
Holocene Sediment Compaction	LARGE QUANTITIES OF RIVERINE SEDIMENT, AS WELL AS DETRITAL AND ALLOCHTHONOUS ORGANIC MATTER, HAVE BEEN DEPOSITED WITHIN THE MISSISSIPPI RIVER DELTA WHERE IT NATURALLY COMPRESSES AND CONSOLIDATES OVER TIME. THE PHYSICAL COMPACTION OF DEPOSITED SEDIMENT IS INFLUENCED BY THE PROPERTIES OF THE SEDIMENT GRAINS, THE VOLUME OF WATER WITHIN THE SEDIMENT, AND THE OVERBURDEN PRESSURE. BIOLOGICAL (E.G., MICROBIAL DECAY OF ORGANIC MATERIAL) AND CHEMICAL (E.G., OXIDATION OF ORGANIC CARBON) PROCESSES CONTRIBUTE TO THE NET EFFECT OF PHYSICAL SEDIMENT COMPACTION THAT PRODUCES SUBSIDENCE, ESPECIALLY IN SOIL CONTAINING SIGNIFICANT AMOUNTS OF PEAT AND OTHER ORGANIC MATTER.
Sediment Loading	ACCUMULATION OF RIVERINE SEDIMENT IN THE MISSISSIPPI RIVER DELTA REGION DURING THE HOLOCENE INDUCED SUBSIDENCE DUE TO FLEXURE WITHIN THE UNDERLYING LITHOSPHERE (I.E., THE CRUST AND UPPER MANTLE). THIS REFERS TO SUBSIDENCE IN THE MATERIAL UNDERLYING A SEDIMENT LOAD RATHER THAN WITHIN THE VERTICAL STACK OF MATERIAL CONSTITUTING THE SEDIMENTARY LOAD.
Glacial Isostatic Adjustment (GIA)	THE LAURENTIDE ICE SHEET THAT EXISTED DURING THE LAST ICE AGE CAUSED CRUSTAL FLEXURE AND SUBSIDENCE. OUTSIDE THE MARGINS OF THE ICE SHEET (E.G., COASTAL LOUISIANA), ISOSTATIC COMPENSATION CAUSED LOCAL UPLIFT AND THE CREATION OF A FOREBULGE. ICE SHEET RETREAT DURING THE HOLOCENE HAS LED TO GRADUAL SUBSIDENCE ALONG THE FOREBULGE. FOREBULGE COLLAPSE OCCURS AT A GEOLOGIC (MILLENNIAL) TIME SCALE. WHILE THE TIMING OF THE COLLAPSE IS DEPENDENT ON THE RATE OF ICE SHEET UNLOADING, THE NATURE OF THE UNDERLYING MANTLE (I.E., THE MANTLE VISCOSITY AND THICKNESS) PRODUCES A SUBSTANTIAL LAG BETWEEN THE TWO.

PROCESS	GENERAL DESCRIPTION
Fluid Withdrawal	AREAS EXPERIENCING WATER AND HYDROCARBON WITHDRAWAL FROM SUBSURFACE RESERVOIRS HAVE BEEN SPATIALLY CORRELATED TO GRADIENTS OF SUBSIDENCE IN SOUTHERN LOUISIANA. FLUID WITHDRAWAL INDUCES A LOSS OF SUBSURFACE PORE PRESSURE WITHIN THE RESERVOIR RESULTING IN LOCAL SEDIMENT COMPACTION, USUALLY IN A ROUGHLY CIRCULAR AREA AROUND THE WITHDRAWAL POINT. REACTIVATION OF FAULT SLIP WITHIN THE NEARBY FAULT ZONES THAT ARE OFTEN ASSOCIATED WITH UNDERGROUND FLUID RESERVOIRS COULD ALSO BE A CONTRIBUTING FACTOR.
Surface Water Drainage and Management	CHANGES IN SURFACE WATER STORAGE AND DRAINAGE PATTERNS INFLUENCE SUBSIDENCE RATES BY ALTERING GRADIENTS OF SOIL MOISTURE. ANTHROPOGENIC MANIPULATION OF THE REGIONAL HYDROLOGY HAS DRASTICALLY ALTERED THE MAGNITUDE AND PATH OF BOTH SURFACE AND SUBSURFACE RUNOFF. DEWATERING OF FORMALLY INUNDATED SOIL INITIATES SEDIMENT CONSOLIDATION AND THE OXIDATION OF SOIL ORGANICS, WHICH REDUCES SOIL VOLUME.

The spatial and temporal scales at which each process influences subsidence can vary (Figure 1). The time scale for analysis in the master plan is 50 years into the future and the spatial scale is coastwide, demonstrating the challenge of considering individual subsidence processes in the analysis. Further, as described by Yuill et al., (2009), subsidence will affect each restoration and risk project differently dependent on the project’s life expectancy and footprint. These temporal and spatial scales and their location within the coastal landscape determine how susceptible different projects, and thus the combination of projects included in the master plan, are to the effects of subsidence.

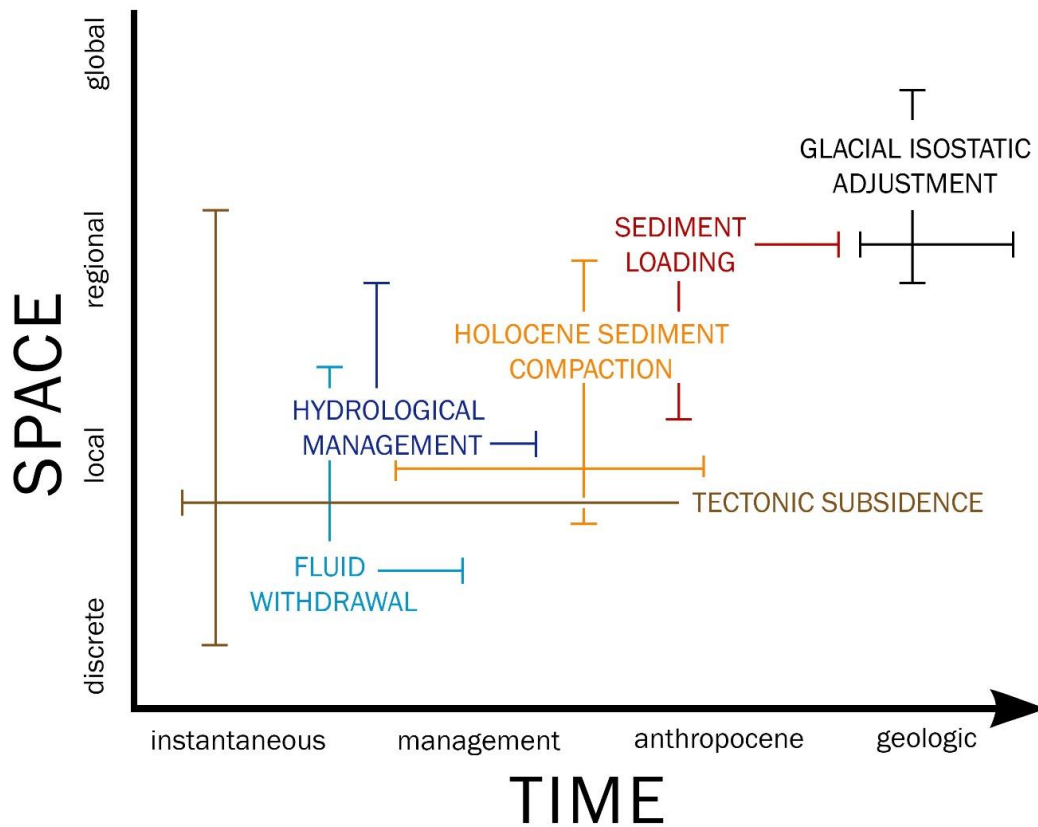


Figure 1. Temporal and spatial scales of the different processes contributing to subsidence. Time scales: instantaneous = 0-1 year, management = 1-20 years, Anthropocene = 20-400 years (for Louisiana), and geologic = >400 years (modified from Yuill et al., 2009).

Contemporary subsidence research employs a wide range of measurement and analytical methods which measure subsidence at different spatial and temporal scales. Commonly used measurement techniques are summarized in Appendix A, Table A1. Each method has its own set of assumptions, levels of precision, and uncertainty. In addition, understanding the range of spatial and temporal scales of various measurement approaches helps identify which subsidence processes are being included within the measurements (Table 1; Figure 1).

Many of the techniques described in Appendix A, Table A1 produce point measurements of subsidence which can limit the utility of the data for purposes such as the development of maps to support master plan analyses. The use of point measurements to infer subsidence rates across broader areas depends on the availability of integrated, complementary data networks (e.g., sediment cores, instruments, or survey benchmarks), as well as confidence in the spatial interpolation of the

point values (Harris et al., 2020). Further, the time scales over which subsidence measurements are made can vary greatly (Figure 2). Some techniques are only applicable for the measurement of specific subsidence processes, whereas others capture several processes.

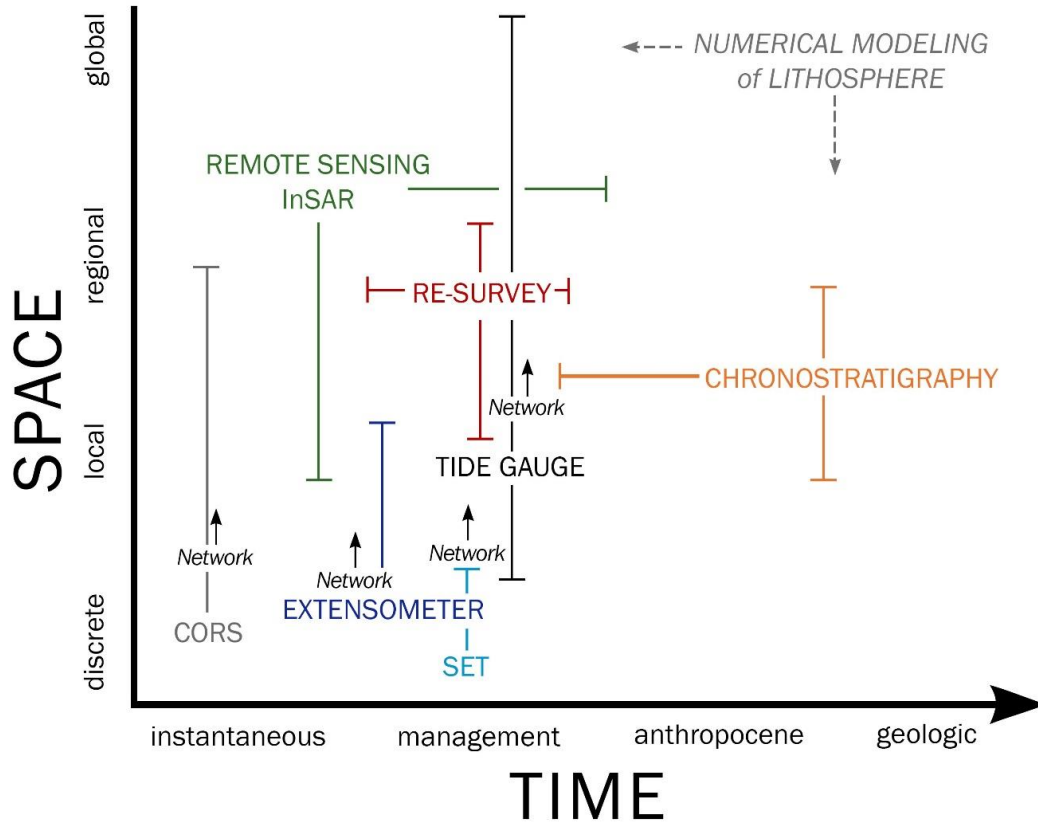


Figure 2. Temporal and spatial scales of various subsidence measurement techniques (modified Yuill, et al., 2009). Additional information about these techniques can be found in Table A1.

2.0 PREVIOUS MASTER PLANS

2.1 SUBSIDENCE IN THE 2012 COASTAL MASTER PLAN

There are many ways to consider unknown future conditions in the context of predictive modeling, and selecting a particular strategy depends on the types of information available and how the results will be used. In the master plan process, the goal of modeling landscape change and storm surge-based flood risk into the future is to provide a way for decision makers to explore the effects of different possible future conditions on the performance of restoration and protection projects. A second goal is to allow for communication with coastal residents about possible future coastal conditions. A scenario approach was used in the 2012 Coastal Master Plan to encompass uncertain future environmental conditions (e.g., future rates of sea level rise). Where there is no known likelihood associated with environmental conditions but rather a range of plausible future conditions, scenario analysis (e.g., Groves & Lempert, 2007; Mahmoud et al., 2009) is useful.

Data limitations prevented the creation of a single coastwide map of subsidence rates to support predictive modeling for the 2012 Coastal Master Plan. Consequently, rates of subsidence were varied across environmental scenarios and ICM outcomes have been impacted at different degrees depending on the particular scenario being used in the model prediction.

For the 2012 Coastal Master Plan, a panel of technical experts was convened to consider available data and determine plausible subsidence ranges for coastal Louisiana (CPRA, 2012). The expert panel convened in 2010 was asked to consider potential driving mechanisms and future rates for different parts of the coast. The process considered information available from previous studies and ongoing work, but was essentially driven by best professional judgement rather than by a comprehensive data analysis. The subsidence rates used for predictive modeling had to be indicative of conditions expected over the next 50 years, which meant assessments of subsidence rates over very short time scales (e.g., sub-annual to annual) could only be used with substantial assumptions.

Through this process, the expert panel decided to develop a map of 17 subsidence sub-regions across coastal Louisiana, each with distinct plausible ranges (Figure 3). For each sub-region, a brief description of its delineation was provided in the 2012 Coastal Master Plan, along with a maximum and minimum rate for future subsidence. These rates vary significantly within and among sub-regions, but in general the lowest rates (as low as 0 mm/yr) are found in areas north of Lake Pontchartrain and in western Louisiana, and the highest rates (up to 35 mm/yr) are found in some impounded areas and the Bird's Foot Delta.

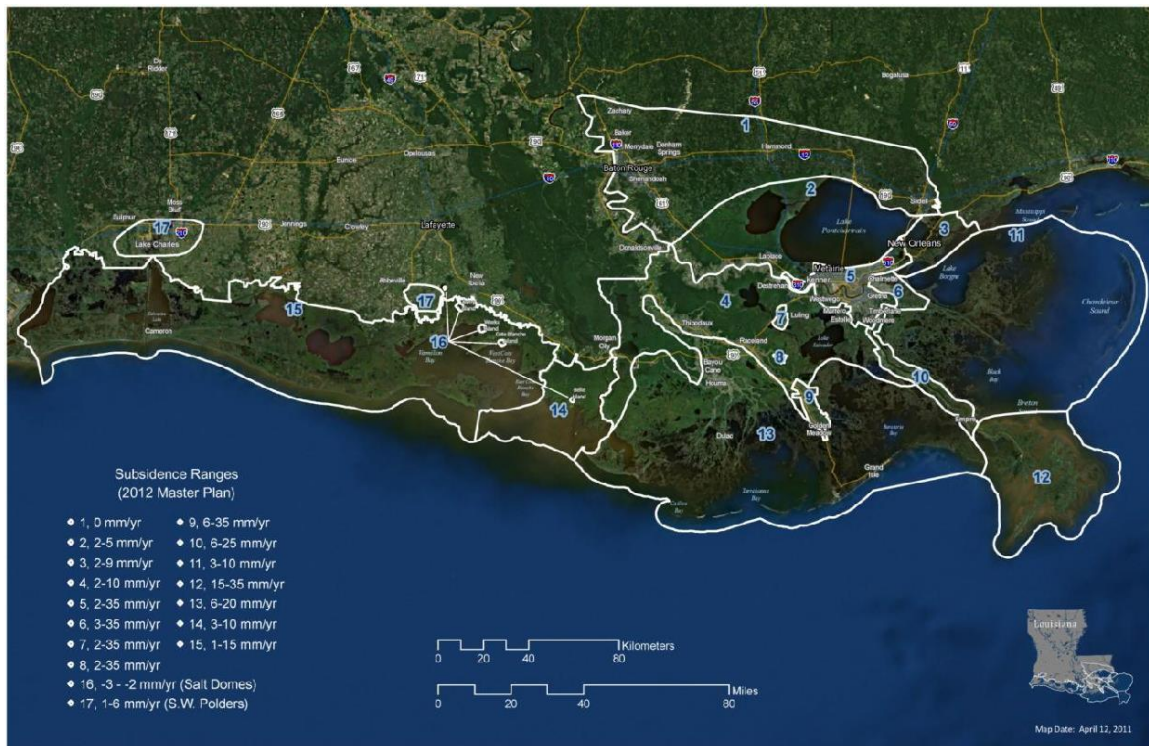


Figure 3. Previously used plausible subsidence rate ranges for coastal Louisiana. These ranges were developed for the 2012 Coastal Master Plan and used in the 2017 Coastal Master Plan.

CPRA selected rates for each sub-region from the ranges determined by the expert panel, with different rates used in different environmental scenarios to represent a variety of possible future outcomes. In the ICM, TS rates applied to each sub-region were calculated using a percentile value for each environmental scenario. Those percentile values were selected by CPRA based on multiple factors:

- For the Moderate Scenario, the 20th percentile value of the range was selected. The rationale for this was that studies published after the 2010 expert panel deliberations suggested subsidence rates could be slowing from higher rates during the mid-20th century, which would make historical rates maximum values.
- For the Less Optimistic Scenario, the 50th percentile was selected. Because of evidence that subsidence rates may be slowing, the mid-range of plausible rates was deemed appropriate to represent a less optimistic scenario.

2.2 SUBSIDENCE IN THE 2017 COASTAL MASTER PLAN

In preparation for the 2017 Coastal Master Plan, CPRA identified and reviewed technical literature developed since the expert panel was convened in 2010. This review was conducted to determine whether improvements could be made to the accuracy and spatial precision of the subsidence values used for master plan analysis by incorporating new data (Reed & Yuill, 2017). Newly available tide gauge data and CORS information was considered. Additionally, new methods of determining subsidence rate in other studies that considered the future of the coastal landscape were reviewed. However, as there were still no definitive studies on subsidence or available data to provide coastwide predictions of future rates, it was concluded that the 2017 Coastal Master Plan should use the same plausible range of subsidence rates by sub-region as used in the 2012 Coastal Master Plan, applied as follows:

- For the Low and Medium Scenarios, the 20th percentile value of the range was selected. This is the same as for the Moderate Scenario from the 2012 Coastal Master Plan.
- For the High Scenario, the 50th percentile was selected. This is the same as for the Less Optimistic Scenario from the 2012 Coastal Master Plan.

3.0 NEW INFORMATION ON SUBSIDENCE RATES SINCE THE 2017 COASTAL MASTER PLAN

During development of the 2017 Coastal Master Plan, an analysis was conducted to characterize both ICM parametric uncertainty and ICM sensitivity to select external drivers such as rates of subsidence and eustatic sea level rise (Meselhe et al., 2017b). This analysis identified that the sensitivity of ICM land area outputs to subsidence rates was of the same magnitude (or greater) than the uncertainties in land area associated with model 'error', as defined by performance statistics generated during the validation process. Given the importance of subsidence rates in determining land loss in the ICM, a reassessment of available studies and data sources was conducted to determine whether predictions of subsidence rates for coastal Louisiana could be refined for the 2023 Coastal Master Plan.

Since decisions on subsidence rates were made for the 2017 Coastal Master Plan, there has been renewed attention to large deltas and coastal populations that are increasingly vulnerable to relative sea level rise. A number of recent studies directly related to measuring subsidence in other coastal areas were reviewed for any insights relevant to the master plan. Several studies examine subsidence in areas with large populations (e.g., Kulp & Strauss, 2019; Syvitski et al., 2009; Takagi et al., 2016). Some studies have focused specifically on estimating subsidence rates using different techniques (e.g., Bekaert et al., 2018 in Sacramento-San Joaquin delta, CA; Grall et al., 2018 in the Ganges-Brahmaputra-Meghna delta; Qu et al., 2019 in Houston; Minderhoud et al., 2018, in the Mekong River delta). Networks of monitoring stations have also been developed in other areas (e.g., Al Mukaimi et al., 2018 notes that the Harris-Galveston Subsidence District established an 80-node network of GPS land deformation monitoring sites).

A number of recent subsidence studies provide rate measurements for specific areas in Louisiana using different techniques and averaging of various time periods. Table 2 summarizes information on subsidence rates from these studies; many include more geographically specific information than is provided below.

Table 2. Summary of information on subsidence rates from recent studies of coastal Louisiana.

PAPER	TECHNIQUE/ APPROACH	TIME PERIOD	GEOGRAPHIC AREA	RATES
Frederick et al. (2019)	CHRONOSTRATIGRAPHY USING BIOSTRATOGRAPHIC DATA IS USED TO DETECT DEEP-SEATED SUBSIDENCE RATES	LATE NEOGENE AND QUATERNARY	COASTAL LOUISIANA AND SHELF	~0.15 – 0.35 MM/YR
Jones et al. (2016)	INTERFEROMETRIC SYNTHETIC APERTURE RADAR (INSAR)	BETWEEN 16 JUNE 2009 AND 2 JULY 2012	LOCAL AREAS WITHIN NEW ORLEANS AND RIVER PARISHES	MICHOUD 15-30 MM/YR U. 9 TH WARD/BAYOU BIENVENUE – 10-20 MM/YR EASTERN METAIRIE 5-15 MM/YR
Yeager et al. (2012)	FAULT OFFSETS USING CHRONOSTRATIGRAPHY	1300 YEARS BEFORE PRESENT (BP) 3700 YEARS BP	LOWER PEARL RIVER VALLEY	A) 1.2 MM/YR B) 0.2 MM/YR
Shen et al. (2017)	FAULT OFFSETS USING CHRONOSTRATIGRAPHY	LATE HOLOCENE LAST GLACIAL LAST INTERGLACIAL	TEPETATE-BATON ROUGE FAULT ZONE	0.22 ± 0.12 MM/YR 0.03 ± 0.05 MM/YR 0.07 ± 0.05 MM/YR
Jafari et al. (2018)*	MODELING OF CONSOLIDATION ASSOCIATED WITH PROJECT IMPLEMENTATION	50 YEARS	CAMINADA HEADLAND	50 CM OVER 50 YEARS
Jafari et al. (2019)*	HIGH ACCURACY ELEVATION MEASUREMENTS OF THE AREAL SUBSIDENCE BENCHMARK	UNDEFINED	CAMINADA HEADLAND	3.38 – 9.27 MM/YR
Karegar et al. (2015)	CORS	4-18 YEARS BP	LOUISIANA	VARIABLE SPATIALLY – UP TO 6.5 MM/YR
Jankowski et al. (2017)	CRMS RSET-MH DERIVED CALCULATIONS OF SHALLOW SUBSIDENCE RATES	2006 THROUGH 2015	COASTAL LOUISIANA	VARIABLE SPATIALLY – MEDIAN RATES OF ~6 MM/YR

PAPER	TECHNIQUE/ APPROACH	TIME PERIOD	GEOGRAPHIC AREA	RATES
Byrnes et al. (2019) [†]	RESURVEY OF CORS AND SECONDARY BENCHMARKS	2003-2019, VARIES BY BENCHMARK	BARATARIA BASIN	0.7-7.1 MM/YR
Byrnes et al. (2015)*	DIFFERENTIAL SEDIMENT CONSOLIDATION ASSOCIATED WITH PROJECT IMPLEMENTATION	FEBRUARY 2013- APRIL 2014 (410 DAYS)	CAMINADA HEADLAND	9.35 MM/YR
*PAPER USES DATA COLLECTED FOR THE PROJECT DESCRIBED IN CAMINADA MOREAU SUBSIDENCE STUDY PHASE 1-3 & PHASE 4 REPORTS PREPARED FOR CPRA BY GAHAGAN AND BRYANT ASSOCIATES, INC.				
† PAPER USES DATA FROM ANALYSIS UNDERTAKEN FOR CPRA BY APPLIED COASTAL RESEARCH AND ENGINEERING (ACRE) ON BARATARIA BASIN. RELATED STUDIES OF BRETON SOUND BASIN (ACRE, 2019) AND TERREBONNE BASIN [N PROGRESS] FOLLOW THE SAME METHODOLOGY.				

For the 2023 Coastal Master Plan approach to determining subsidence rates for use in predictive modeling, studies that compile data from across the coast representing different processes and use it to quantify rates and use averaged rates across variable time periods are of particular interest. One such study, Jankowski et al. (2017), uses RSET-MH data from the CRMS network, with limited CORS benchmark data, to estimate SS rates across coastal Louisiana wetlands and note complex patterns of both SS and apparently, in some instances, net surface elevation increase. Median rates of SS from that study are 6.0 mm/yr for the Mississippi Delta and 5.8 mm/yr for the Chenier Plain.

CPRA previously compiled elevation time series data for GPS benchmarks within the Barataria Basin (Byrnes et al., 2019) and the Breton and eastern Pontchartrain Basins (ACRE, 2019). The Barataria Basin analysis includes five CORS primary benchmarks, and 14 CPRA/National Geodetic Survey (NGS) secondary benchmarks, while the Breton and Pontchartrain Basin analysis includes 11 CPRA/NGS secondary benchmarks. Historical raw GPS datasets (i.e., Receiver Independent Exchange Format files) for the secondary benchmarks between 2003 and 2019 were processed, and linear regression was used to calculate subsidence rates (elevation change with time) associated with elevation measurements for the survey locations in the basins. The geodetic measurements in Barataria, Breton and eastern Pontchartrain basins documented subsidence rates ranging from 0.7 to 7.1 mm/yr (Byrnes et al., 2019; ACRE, 2019). This type of analysis is currently being repeated for coastal basins to the west.

There is ongoing discussion (Cahoon et al., 2020) of what the subsidence rates measured using the RSET-MH method and benchmark resurvey data represent in terms of substrate process contributions to subsidence. Byrnes et al. (2019) propose that unless rods are sleeved it is unreasonable to assume that they are not impacted by subsidence in the surrounding substrate (i.e., they are subject to down

drag). Thus Byrnes et al. (2019) assume that the subsidence they calculate based on the resurvey of un-sleeved benchmarks represents TS. However, there have been no direct estimates of such down drag on RSET rods in Louisiana. Swales et al. (2016) used standard geotechnical engineering methods to estimate the bearing capacity (i.e., skin friction resistance) of an RSET benchmark in the Firth of Thames sedimentary basin, relative to the force exerted by the benchmark mass, and the potential point settlement. The potential settlement of the RSET benchmarks in the substrate was estimated as $\sim 2.6 \times 10^{-5}$ m (~ 0.03 mm) from the general sediment properties (assuming stiff clay) and the benchmark properties.

Further research is needed to improve understanding of the processes that each technique measures, including geotechnical measurements of potential down drag using information on Louisiana substrates. However, the benchmark resurvey and RSET-MH data sets currently provide the best opportunity to capture deep and shallow contributors to subsidence coastwide and to characterize TS based on data collected using consistent methodologies.

4.0 SUBSIDENCE APPROACH FOR THE 2023 COASTAL MASTER PLAN

4.1 APPROACH

Building on reported measurements of subsidence from several recently available studies (see Section 3.0), subsidence can be divided into two separate rates that can be treated additively in master plan modeling (Figure 4):

- DS rates based on data from 5-15 year GPS records and repeated geodetic surveys of deep-seated monuments (CORS and secondary benchmarks) across coastal Louisiana, and
- SS rates based on available 10+ year RSET-MH measurements at CRMS and other sites, characterizing shallow processes in wetland settings.

These two rates are used collectively to characterize spatial variation in subsidence reflecting the entire sediment column. By using both data sets, the master plan analysis can incorporate the effects of a broad array of subsidence processes (Figure 1, Table 1), and how they impact the performance of different restoration and protection projects considered for the master plan. The rates from these data sources can be compared to rates from other methodologies in the same geographic area to determine confidence in the component rates, for example from studies listed in Table 2 and others previously summarized (e.g., by Yuill et al., 2009; Reed & Yuill, 2017).

A composite map of TS, developed by combining separate maps of DS and SS created using available data, provides greater spatial variation in subsidence rates across the coast than the sub-region approach used in previous master plans. The assumptions used in developing these maps and the limitations of the maps are discussed below.

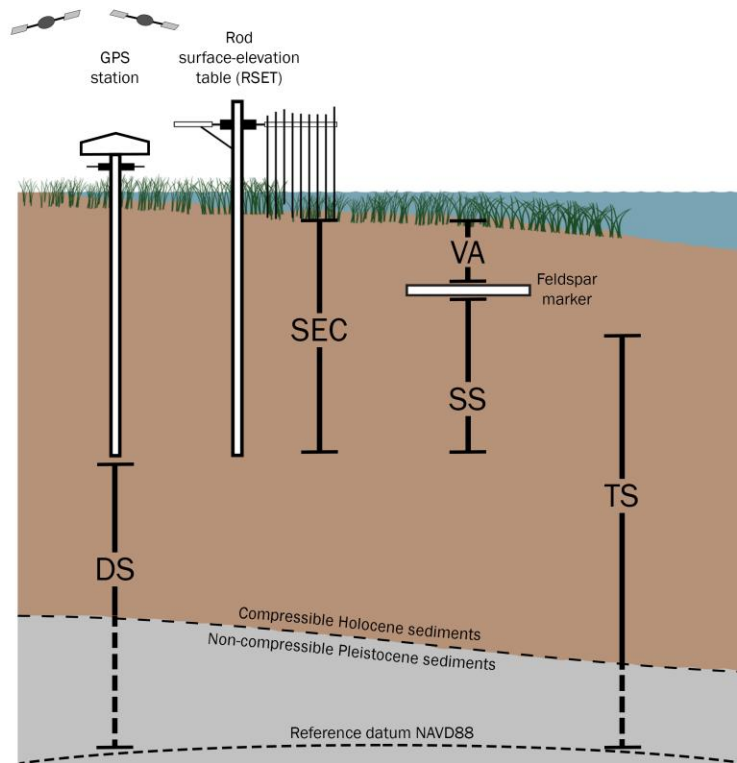


Figure 4. Representation of measurements used to develop subsidence rates for the 2023 Coastal Master Plan. Note that objects and distances in the figure are not to scale. Figure modified from Cahoon et al., 2006 and Jankowski et al., 2017.

4.2 ASSUMPTIONS AND LIMITATIONS

The approach to developing a TS map as an additive map of DS and SS is subject to a number of assumptions. Assumptions associated with specific aspects of the data used for DS and SS respectively are described in sections below. It is also important to note that since surficial processes of organic matter accumulation and mineral sediment deposition are accounted for separately in the ICM (White et al., 2017), they are not included in the subsidence estimates developed to support the 2023 Coastal Master Plan.

One of the assumptions underlying the approach is consideration of temporal variations. The data from benchmark resurveys or CORS stations only track change over periods of 5-15 years due to the duration of available records. RSET-MH records are also only available since 2006. Thus, the

assumption is made that these relatively short-term measurements appropriately represent processes that occur over multi-decadal time scales and adequately represent subsidence conditions for the entirety of the 50-year master plan analysis period. Further, linear regressions (see details below) are used to develop subsidence rate estimates for both data sets. Because of the multiple contributing processes to both deep and shallow subsidence, there is the potential for non-linear effects in one or more contributions. Data sets were considered too short to provide meaningful tests of non-linearity in the data. Studies with data covering much longer periods (Frederick et al., 2018), have interpreted periodic movements of faults over time but this would require very detailed spatial resolution to identify locations and additional assumptions about the temporal frequency of faulting to include in a 50-year analysis.

Mapping of subsidence surfaces based on point data also requires spatial interpolation or spatial aggregation into regions or polygons. As described below, different spatial assignment techniques were used for deep and shallow subsidence. This is based on the assumption that DS is driven by processes controlled by larger scale geologic facies distribution and underlying structures, thus rapid transitions in rates over small distances are not the norm (see Section 5 for exceptions).

In contrast, while potential contributing processes for SS have been documented in different studies (see Section 6), how these processes vary spatially based on their relative contributions is not well understood. Complex patterns of variation in SS rates among CRMS sites have been documented (Jankowski et al., 2017) and may be in response to local variations in substrate dynamics, e.g., excessive drainage, or variations in organic matter contributions by plant species and thus, consistent patterns are not necessarily expected.

Ideally, the derivation of SS and DS rates based on monuments distributed across the coast would use the same monuments for both sets of measurements. However, while some of the secondary benchmarks are located in the vicinity of CRMS sites, the benchmarks are not the actual RSET rods. Approaches have been developed to utilize RSET rods for geodetic survey and connection to the National Spatial Reference System (Geoghegan et al., 2009), but thus far this has not been widely applied in Louisiana. Thus, the benchmark surveys used to derive DS measurement and the RSET-MHs used for the SS measurements may either not encompass the entire subsurface profile, or may both consider part of the same profile (e.g., if the RSET penetrated deeper than the benchmark monument or vice versa). Foundation data for the benchmarks and the RSET rods were used to assess the relative importance of this aspect of the additive assumption.

Two natural neighbor interpolated surfaces were developed for the foundation depths for both the DS and SS data sets. The DS foundation depth surface was subtracted from the SS foundation depth surface, allowing them to be compared while accounting for the lack of spatial continuity and the differences in the number of sites. The difference between these two surfaces (Figure 5) represents the estimated degree of vertical overlap or separation of the monuments. The resulting difference map shows that for most of the western part of the coast, foundation depths for benchmarks are

deeper than for RSET rods (negative values in Figure 5). This means that subsidence occurring over part of the substrate (over 3 m in some areas) is not considered by the analysis presented here. In contrast, in the southeastern part of the coast RSET rods may be anchored more than 10 m deeper than the benchmark foundations. This leads to a potential miscounting of the component contributions of processes occurring within the overlapping section of the sediment column that would artificially increase the rate of subsidence locally. The consequences of these differences will be discussed in relation to the TS rates in Section 7.0 of this report.

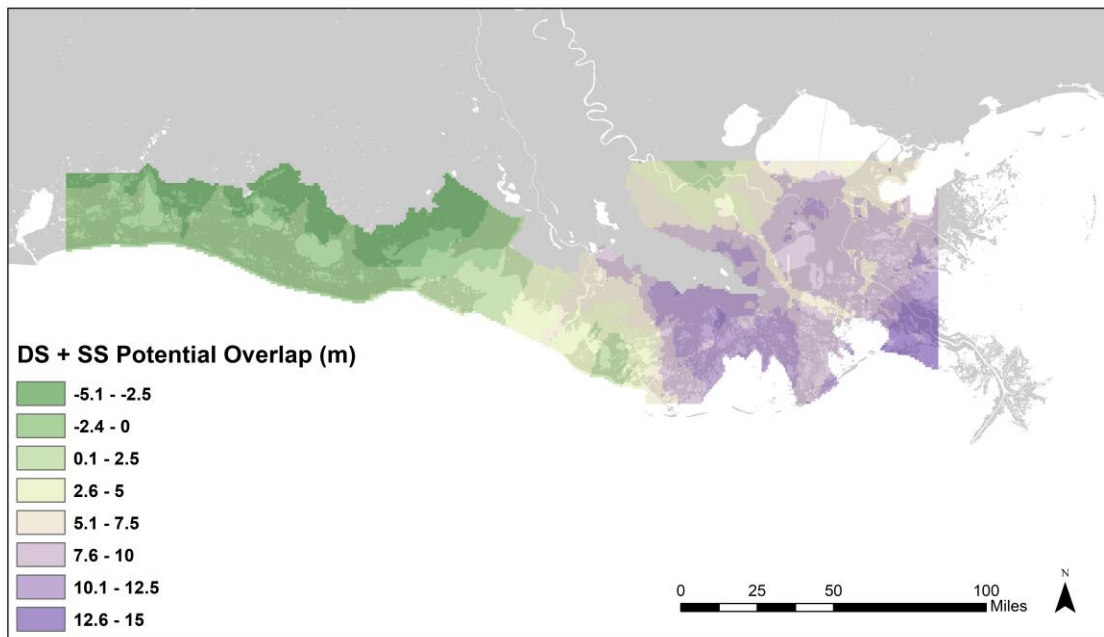


Figure 5. Potential overlap of DS and SS in meters developed through surface differencing. Differences in the foundation depth of CRMS site RSET rods and CORS sites or secondary benchmarks are shown. Negative values (greens) indicate a gap between the two foundation depths, which could produce an underestimate in calculated TS. Positive values (purples) indicate that there is overlap of the two foundation depths, which could produce an overestimate in calculated TS.

5.0 DEVELOPMENT OF A DEEP SUBSIDENCE MAP FOR COASTAL LOUISIANA

5.1 DEEP SUBSIDENCE DATA

As described in Appendix A, Table A1, primary CORS benchmarks and secondary CPRA/NGS GPS benchmarks are permanent fixtures. Both benchmark types are anchored at depth and measurements are made with respect to a known vertical datum. Repeating GPS measurements of the vertical location of a benchmark over time can provide time series data of vertical motion. While both measurement techniques provide point measurement of subsidence at a fixed location, CORS networks provide continuous records of the three-dimensional GPS position of a given benchmark (Karegar et al., 2016). In contrast, acquisition of data from secondary benchmarks requires re-surveying of the site and the resulting time series represents the change in vertical location with respect to a known vertical datum over time. Fundamentally, however, the two methods have key similarities that allow the subsidence rates measured by each to be considered comparable.

With both methods, the measurements of vertical motion obtained encompass a number of processes that, in general, act on long (centennial to millennial) time scales (Figure 2). Additionally, the assumption is made in this approach that these methods record movement from the base of the benchmark anchor and below as that is the fixed vertical reference point for the site (see discussion above). This motion is attributable, in part, to deep-seated tectonic processes such as fault slip in active fault zones and motion related to salt intrusion (Keogh & Törnqvist, 2019). Additionally, these DS rates include the deep component of Holocene compaction (where benchmarks are anchored in Holocene sediments), sediment loading resulting from delta building processes, and the resultant downward flexure of the underlying lithosphere (Blum et al., 2008). The process of GIA also contributes to the DS rate (Gonzalez & Törnqvist, 2006; Sella et al., 2007). Fluid withdrawal from deep substrates, such as that associated with oil and gas production, may also locally contribute to DS (Morton & Bernier, 2010).

The approach described in this report relies on data available as a result of several new studies (Karegar et al., 2016; ACRE, 2019; Byrnes et al., 2019). While these studies cover eastern basins, they have not yet been extended to the west. For parts of coastal Louisiana lacking data from these studies, vertical displacement measurements were supplemented through additional analysis by the CPRA team using a similar methodology.

5.2 DETERMINING DEEP SUBSIDENCE RATES

For the 2023 Coastal Master Plan subsidence approach, DS mapping incorporates geodetic survey data from across coastal Louisiana. This data (Appendix B, Table B1) represents both a comprehensive re-analysis of CORS and secondary benchmark data from Barataria, Pontchartrain, and Breton Sound basins (ACRE, 2019; Byrnes et al., 2019), as well as a supplementary analysis of CORS and secondary benchmarks for basins west of Barataria (Figure 6). Estimated values of 0.5 mm/yr were used for the North Shore of Lake Pontchartrain in areas where no benchmark data were available. Selection of primary and secondary benchmarks for the supplementary analyses (Table B1) was based on availability of suitable data and coastwide spatial distribution of the selected benchmarks. Benchmarks within the model domain were omitted if they had less than 1 cm of vertical change during the period of observation (following the method of Byrnes et al., 2019), as elevation measurements were made to an accuracy of less than 1 cm.

For benchmarks in Barataria, Pontchartrain, and Breton Sound basins, DS rates were taken directly from ACRE (2019) and Byrnes et al. (2019). To characterize subsidence outside these basins estimates of DS were derived from 5-14 year long records at 3 primary and 14 secondary benchmarks. Vertical displacement from the initial benchmark survey and the most recent survey data available were calculated to provide DS estimates for the remaining parts of the coast. Most observations in the western basins consisted of only two observation points per station and could not be statistically analyzed to determine the fit of the rate to the data.

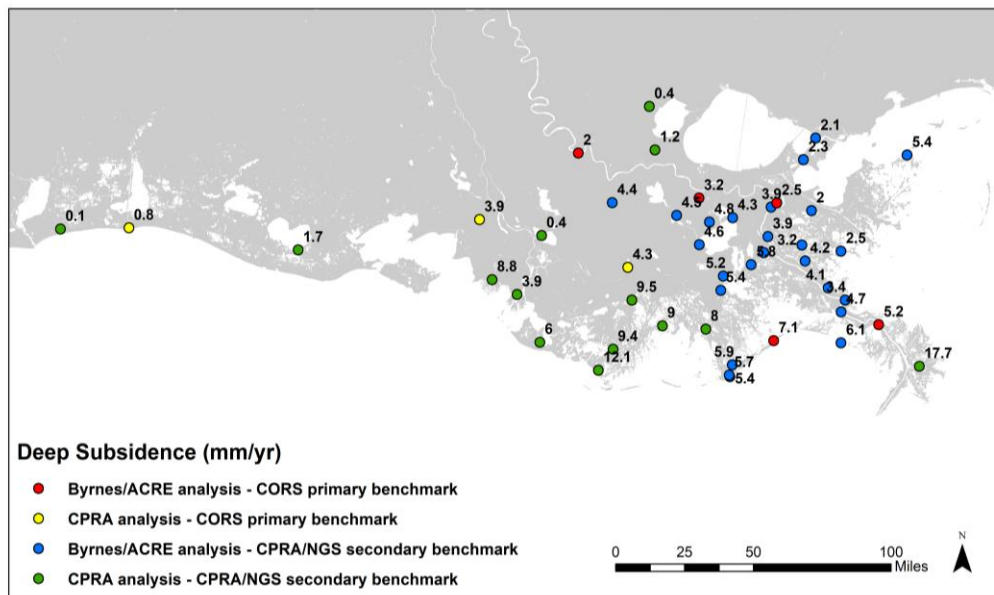


Figure 6. Coastwide deep subsidence point data, including the source for benchmark analysis.

Within Barataria basin, DS rates ranged from 2 to 7.1 mm/yr and in Breton and eastern Pontchartrain basins rates ranged from 2.1 to 5.9 mm/yr (Appendix B, Table B1; Figure 6). To characterize subsidence outside of the area considered by ACRE (2019) and Byrnes et al. (2019), estimates of DS were derived from 5-14 year long records at 3 primary and 14 secondary benchmarks by calculating the difference from initial and most recently reported vertical displacement rates. Previous research suggests subsidence in the Chenier Plain is primarily a function of GIA rather than sediment loading (Yu et al., 2012; Blum et al., 2008). Wolstencroft et al., (2014) characterizes GIA-derived subsidence rates, measured at roughly ~1 mm/yr, as the lower bound of total Chenier Plain subsidence. The supplementary benchmark analysis included here confirm these rates, ranging from 0.1 near the Sabine River to 1.7 mm/yr south of White Lake (Appendix B, Table B1; Figure 6).

The North Shore of Lake Pontchartrain was not formed by the same deltaic processes as the Mississippi River Delta plain to the south and has a relatively thin Holocene sediment package (Kulp et al., 2002). The 2010 subsidence expert panel estimated a subsidence rate of 0 mm/yr for that area, which was applied for the 2012 and 2017 Coastal Master Plans. Only one secondary benchmark with appropriate survey data was available west of Lake Maurepas. It had a subsidence rate of 0.4 mm/yr (Appendix B, Table B1; Figure 6). While DS is considered minimal on the North Shore, observed vertical displacement attributed to fault activity has been observed in some locations (Yeager et al., 2012; Shen et al., 2017; Table 2) and therefore should not be entirely omitted. Subsidence rates of 0.5 mm/yr are assumed to characterize this portion of the coast.

5.3 SPATIAL APPLICATION OF DEEP SUBSIDENCE

There are a number of methods available to interpolate point data to create a continuous surface of DS rates for the 2023 Coastal Master Plan. Selection of an interpolation method is based upon the characteristics of the underlying data and an understanding of inherent spatial relationships between data points. In the Mississippi River delta plain there is substantial variation in the thickness of Holocene deposits and time since deposition, with thicker sediment packages and younger deposits contributing to higher rates of DS (Törnqvist et al., 2008). The depth of the Pleistocene surface (and therefore thickness of Holocene sediment package) in the Mississippi River delta plain generally increases toward the Gulf of Mexico and varies laterally, especially in relation to the underlying incised alluvial valley (Kulp et al., 2002).

Given these interacting patterns and the complexity of the contributing processes, a map of DS in coastal Louisiana was developed using natural neighbor interpolation (Figure 7). The map creates a continuous surface of DS rates across coastal Louisiana based on data availability, as opposed to dividing the coast into sub-regions with distinct subsidence rate ranges (as for the 2012 and 2017 Coastal Master Plans). The natural neighbor method was selected to interpolate point data because it is a distance-weighted interpolation method: the closer an input point is to the location of an output cell, the greater influence the input point has on determining the output cell value (Childs, 2004). This approach assumes that DS is a function of regional variations in underlying geology, thus subsidence

rates in closer proximity will be similar as a result of common geologic processes, whereas rates may be more variable where points are more widely spaced. This assumption diminishes the potential role of features such as paleochannels on local variations in subsidence. More detailed spatial data would be needed to include such effects.

Figure 7 shows the resulting interpolated DS surface. The Chenier Plain largely shows DS rates up to 1.5 mm/yr. DS rates of less than 3 mm/yr are also found on the North Shore of Lake Pontchartrain and areas east of New Orleans. Along the coast, rates of 4.5-6 mm/yr are shown in the Teche-Vermilion area. For the Mississippi River delta plain rates range from 4 mm/yr to ~17 mm/yr. The highest DS rates in coastal Louisiana occur in the lower basins, with rates up to 12 mm/yr throughout lower Terrebonne Basin, up to 7.5 mm/yr in lower Barataria Basin and outer Breton Sound Basin, and up to 17 mm/yr in the Bird's Foot Delta. Additional information regarding the underlying DS data can be found in Appendix B, Table B1.

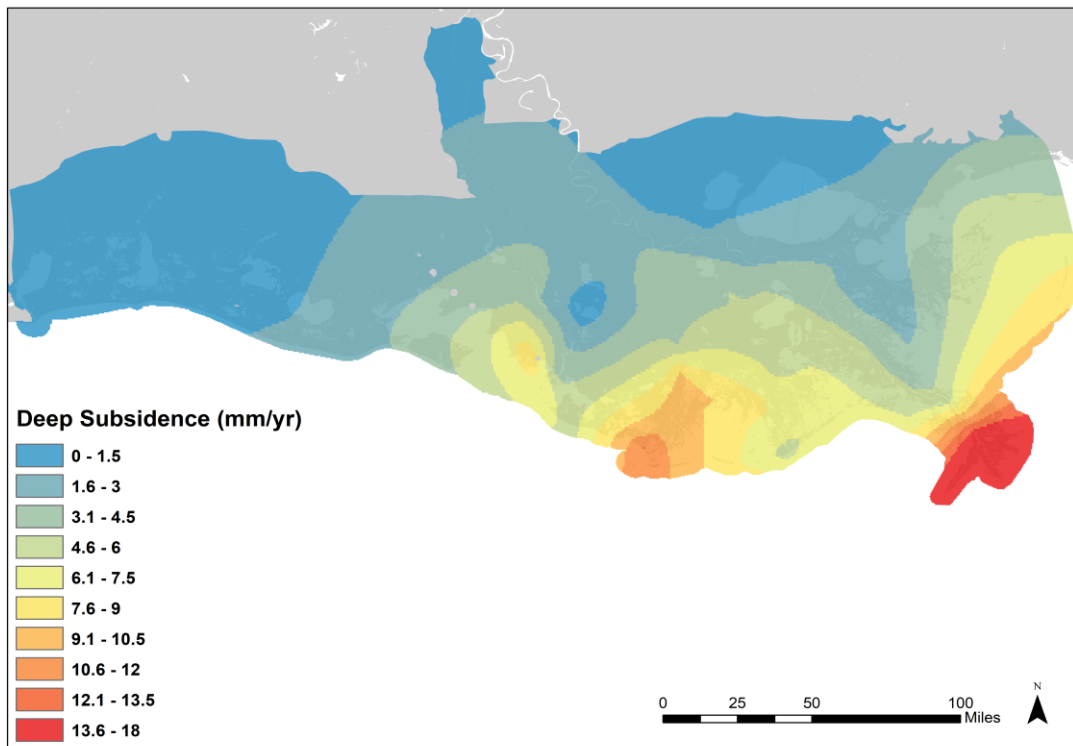


Figure 7. Deep subsidence map of coastal Louisiana. Interpolated surface using the natural neighbor method from point data (see Figure 6).

5.4 ASSUMPTIONS AND LIMITATIONS OF DEEP SUBSIDENCE APPROACH

Without higher-resolution measurements of DS rates across the coast, the development of a subsidence map will always be subject to assumptions. This map is specifically designed to be used with the map of SS (see below) to produce subsidence rates for use in coastwide predictive land change and storm surge modeling for the master plan. It is not intended for use in design or operation of coastal restoration and protection projects that require site-specific information. The intent is to show broad spatial patterns generally representative of measured values for DS. Specific defined geological features that result in distinct differences in DS, e.g., the salt domes in Figure 3 (region 16) that show uplift, are omitted from the subsidence domain used for the modeling. This may lead to a slight overestimation of storm surge-based flooding in these areas, as uplift over 50 years would not be taken into account, but the effects are likely to be minimal as the uplift rates estimated previously were only 2-3 mm/year (Figure 3) and the salt domes identified are relatively high elevation features.

Deep subsidence rates were developed for application across predictive models including landscape (ICM), storm surge (ADCIRC), and risk assessment (CLARA). More information about the application of subsidence rates in these models can be found in their respective appendices.

There is ongoing scientific discussion as to whether the term ‘deep subsidence’ is applicable to these data. Frederick et al. (2019) note that ‘deep-seated’ subsidence includes processes such as growth faulting, lithospheric flexure, and long-term compaction that operate at the regional scale. This approach considers these as contributing processes, along with others that influence the lowering of benchmarks. Thus, the definition here is more measurement-based than process-based. By considering that lowering of benchmarks represents DS as opposed to TS, this approach follows that from Cahoon et al. (2020) and differs from that proposed by Byrnes et al. (2019). The section below on SS further clarifies the distinction made for the approach to representing total subsidence rates in the ICM.

While the DS data considered here are derived from consistent measurement approaches, there is some difference in how sub-groups of that data have been analyzed. The detailed reanalysis of previous benchmark surveys conducted by Byrnes et al. (2019) was not applied to all secondary benchmark data used here. Extensive height modernization efforts were undertaken by the NGS¹, including updates to the reference geoid used. In addition, surveys were conducted by a variety of institutions or contractors potentially resulting in slight differences in data analysis. Detailed reanalysis of the original survey files would be needed for the secondary benchmark information to be more consistently used in this analysis. As previously noted, this work is underway for some parts of the coast, and subsidence rates at specific benchmarks can be updated for future coastal master plans

¹ <https://www.ngs.noaa.gov/heightmod/GulfCoastProject.shtml>

as information becomes available.

In addition, the limited distribution of benchmarks and monuments requires extensive interpolation of data. This is the case in almost any geological mapping that is based on point data sets (e.g., Karegar et al., 2015). Few subsidence studies can match the density of measurements in the borehole data used by Frederick et al. (2019). Their data however, are less useful for the purpose of master plan predictive modeling due to the limited resolution of onshore data representing recent (i.e., in the last millennium) motion.

6.0 DEVELOPMENT OF A SHALLOW SUBSIDENCE MAP FOR COASTAL LOUISIANA

6.1 SHALLOW SUBSIDENCE DATA

A coastwide map of SS rates was developed using RSET-MH data from 203 CRMS sites and non-rod SET data from a recent study by Lane et al. (2020). For the purposes of this report, SS is defined as the difference between the observed rates of vertical accretion (VA) and surface elevation change (SEC) (Figure 4; Cahoon et al., 1995). While trends of VA and SEC coastwide are positive, in most cases, VA outpaces SEC. This difference indicates that processes in the near subsurface contribute to the lowering of the land surface, negating some of the contribution of VA. VA is accounted for dynamically in ICM-Morph, so separately accounting for SS and DS allows the ICM to track multiple factors influencing wetland elevation change within the ICM.

The measurements of SS obtained using RSET-MH methods encompass a number of processes that are not entirely independent (e.g., Morris et al., 2002) and demonstrate significant spatial variability (Jankowski et al., 2017). This methodology for determining SS estimates vertical changes between the base of the RSET rod (the datum for the SEC measurements) and the base of the MH (the datum for the VA measurements) (Cahoon et al., 1995). Several studies have suggested that such measurements include the majority of modern compaction occurring near the surface of the Holocene sediment package (Meckel et al., 2006; Jankowski et al., 2017).

In coastal Louisiana, the processes encompassed by SS rates include biological processes such as organic matter decomposition and primary production (e.g., Kirwan & Guntenspurgen, 2012) and geomorphological processes such as shallow Holocene sediment consolidation and compaction (Törnqvist et al., 2008). Anthropogenic sources of subsidence, including surface water level management and subsequent compaction, may also contribute to SS (Yuill et al., 2009). When occurring in the shallow subsurface in areas proximal to RSET-MH measurements at depths above the rod depth, these sources of subsidence would also be accounted for here.

6.2 DETERMINING SHALLOW SUBSIDENCE RATES

For this analysis, SS is defined as the net vertical displacement resulting from the processes that occur above the foundation depth of the monument used to measure SEC (i.e., the RSET) and below the MH used to measure accretion (Figure 4). Note that as for DS, the definition here is more measurement-based than process-based. Monuments for the purpose of this study are RSETs

installed at varying depths (average depth of around 20 m at CRMS sites), although some data from Lane et al. (2020) using non-rod SETs (Cahoon et al., 2002) have been used to ensure coverage in areas where CRMS data is limited. SEC is the change in the elevation of a marsh or surface as measured by the RSET, and VA is the thickness of material above a feldspar MH, usually measured using cryogenic coring (Cahoon et al., 1996). The rate of SEC is subtracted from the rate of VA at each site to determine SS:

$$SS = VA - SEC \quad \text{[EQUATION 1]}$$

The methodology for determining SS in the report follows the approach used by Jankowski et al. (2017), though additional time series data and additional CRMS sites are included in this analysis. At each CRMS site (except float sites), SEC and VA were measured and recorded, usually semi-annually during Spring and Fall for SEC and annually for VA. Marker horizons were established progressively (Table 3) to ensure detection of markers could be maintained over time and each CRMS site has several established plot sets surrounding the RSET. Measurements are made at each CRMS site by plot set (where each plot set consists of three marker horizons, 0.5 m x 0.5 m). When a new plot set is deployed it is measured twice per year, while plot sets older than two years are measured every one and a half years.

Table 3. Plot Set Sampling Years. Ranges of years indicate the observation window for the plot set.

PLOT SET	YEARS
1	2008-2018
2	2010-2019
3	2012-2018
4	2014-2018
5	2016-2019
6	2018-2019

SEC and VA data from plot set 1 were selected for this analysis as plot set 1 has the longest continuous record, enabling the consistent assessment of SS rates over time. Additionally, comparison of VA rates from plot set 1 versus plot set 2 data showed very little difference. VA and SEC sample dates were converted to decimal year, and a linear regression was applied to both data sets to determine a VA rate and an SEC rate (Figure B2). Equation 1 was then applied to yield the SS rate.

Not all CRMS site records were used in this analysis; CRMS sites were omitted for the following reasons:

- Either the VA or SEC data sets had less than 5 observations,
- VA or SEC data sets had high inter-annual variability (low coefficient of determination for linear regressions),
- The SS rate at a station was greater than 2 standard deviations outside of the overall average SS rate, potentially indicating that local conditions were influencing either VA or SEC, and/or
- Sites were identified as experiencing shoreline erosion or as floating marsh sites at any point throughout the observation period or by CRMS field operators.

The remaining SS rates from CRMS sites that met data criteria are shown in Figure 8. Specific point data for all CRMS sites can be found in Appendix B, Table B2.

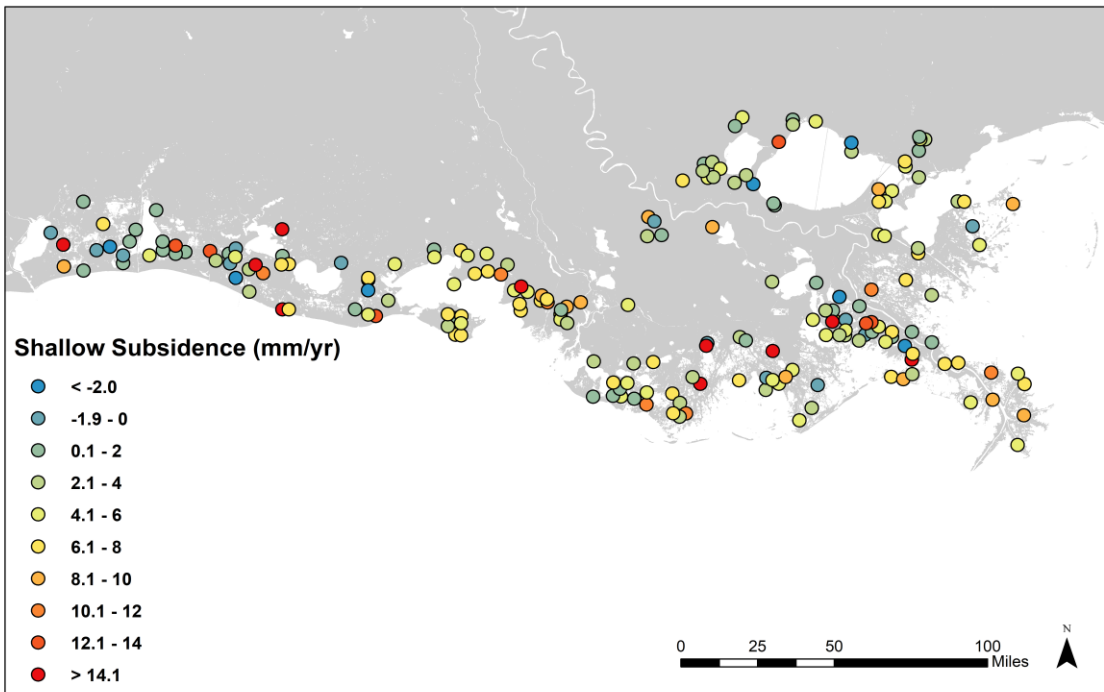


Figure 8. Shallow subsidence RSET-MH point data from 203 CRMS sites. Not included in the figure are additional points of non-rod SET data from the eastern Pontchartrain basin. A full table of shallow subsidence point values can be found in Appendix B, Table B2.

6.3 SPATIAL APPLICATION OF SHALLOW SUBSIDENCE

SS point data shows high spatial variability (Figure 8) similar to that identified by Jankowski et al. (2017). As much is still unknown about the processes contributing to SS across the coast (see Section 6.4), it was determined that uncertainty in the spatial and temporal accuracy of SS rates across the coast was too great to apply spatially interpolated SS point data over a 50-year model simulation. However, it seems reasonable to assume that there are regionally-related variations in the processes that drive SS, such as vegetation type and hydrology.

The analysis for the 2023 Coastal Master Plan already uses a series of 25 ecoregions to summarize select model outputs for use in decision making (Figure 9), identified based on major hydrologic boundaries. As SS is at least in part hydrologically influenced, SS rates were aggregated by ecoregion and summary statistics were performed for each ecoregion. Note that the additional non-rod SET data from Lane et al. (2020) was included in the aggregation and calculation of summary statistics in the eastern Pontchartrain ecoregions, as few CRMS sites exist in those ecoregions. To account for both potential overlap in SS and DS processes (Figure 5) and for uncertainty in SS rates over time, two SS maps (see Section 7.3) were developed by taking the first quartile and median of aggregated shallow subsidence rate point values by ICM ecoregion (Table 4; Figure 10 and Figure 11). Ecoregions with fewer than two points were aggregated into a neighboring ecoregion. The first quartile and the median SS ecoregion values each added to DS map create two total subsidence maps representing a lower and higher subsidence scenario, respectively (see Section 7.3).

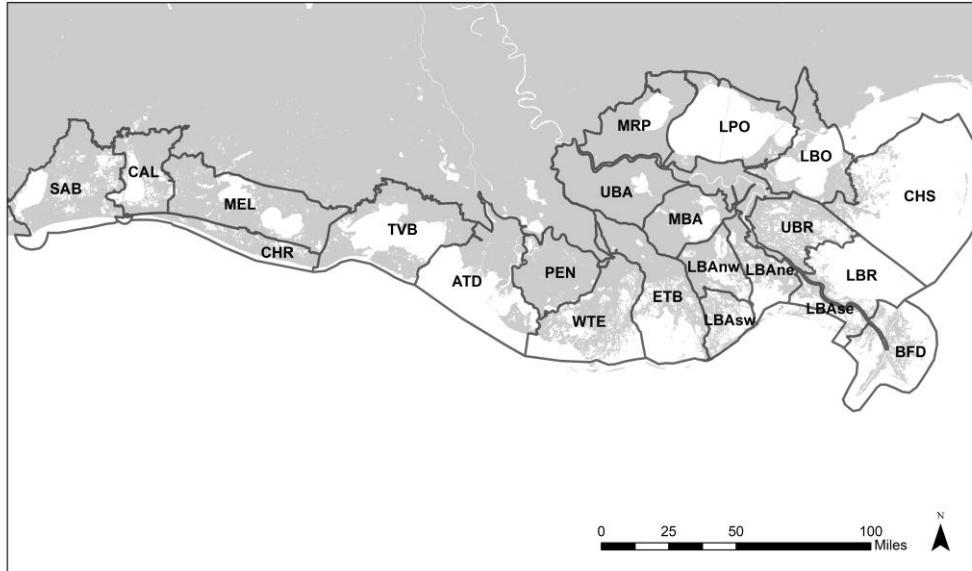


Figure 9. Map of 25 ecoregions defined for the 2023 Coastal Master Plan. Ecoregions used to aggregate data for the shallow subsidence surface map.

Table 4. Aggregated shallow subsidence statistics and values by ecoregion. Ecoregions highlighted in the same color were combined.

ECOREGION		FIRST QUARTILE	MEDIAN
ATB	Atchafalaya Basin	NO DATA	NO DATA
ATD	Atchafalaya Delta	5.4	7.2
BFD	Bird's Foot Delta	4.8	7.3
CAL	Calcasieu	0.6	1.0
CHR	Chenier Ridges	4.0	6.6
CHS	Chandeleur Sound	2.9	6.9
ETB	Eastern Terrebonne	3.0	4.5
LBAne	Lower Barataria (NE)	0.7	2.7
LBAnw	Lower Barataria (NW)	2.5	3.9
LBAse	Lower Barataria (SE)	5.8	6.6
LBAsw	Lower Barataria (SW)	2.5	3.9
LBO	Lake Borgne	1.9	3.1
LBR	Lower Breton	5.3	6.6
LPO	Lake Pontchartrain	1.7	2.9
MBA	Mid Barataria	1.1	2.4
MEL	Mermentau/Lakes	0.2	3.9
MRP	Maurepas	2.7	3.9
PEN	Penchant	3.2	5.6
SAB	Sabine	-0.6	1.1
TVB	Teche/Vermilion/Bays	4.2	5.5
UBA	Upper Barataria	1.1	2.4
UBR	Upper Breton	3.7	6.5
UVR	Upper Verret Basin	NO DATA	NO DATA
VRT	Verret Basin	NO DATA	NO DATA
WTE	Western Terrebonne	2.0	4.3

As the analysis is based on data collected within coastal wetlands, it is unknown how much SS may be occurring in sediments underlying the coastal bays. The bottoms of most bays are shallower than the ~20 m depth of the RSET monuments, and thus some of the substrate underlying the bays is at a

similar subsurface 'depth' to the wetland substrate considered in the SS calculations. By not extending the SS domain to the coastal bays, the approach assumes that these are only subject to DS. This may lead to some underestimation of TS in the bays (see Section 7).

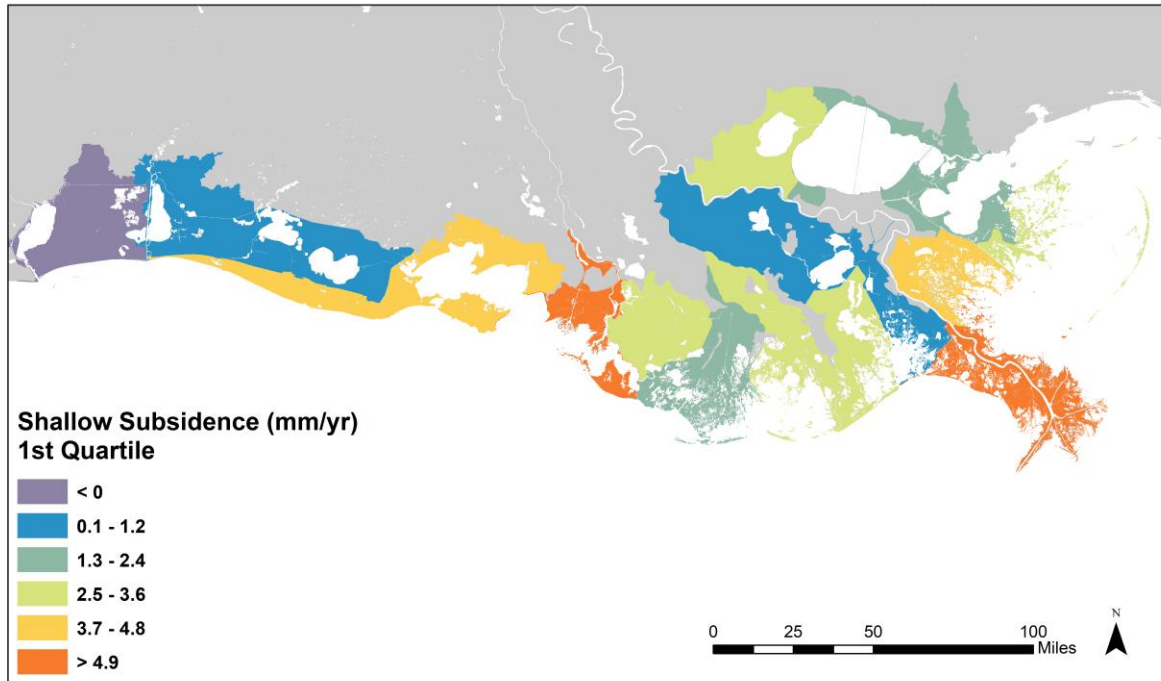


Figure 10. First quartile of shallow subsidence rate point data aggregated by ecoregion across coastal Louisiana. The map includes point data for shallow subsidence measured at 203 CRMS sites. Ecoregions with less than 2 points were aggregated into a neighboring ecoregion. Eastern Pontchartrain includes data from Biloxi Marsh SET data. Some smaller water bodies may not be represented on the map.

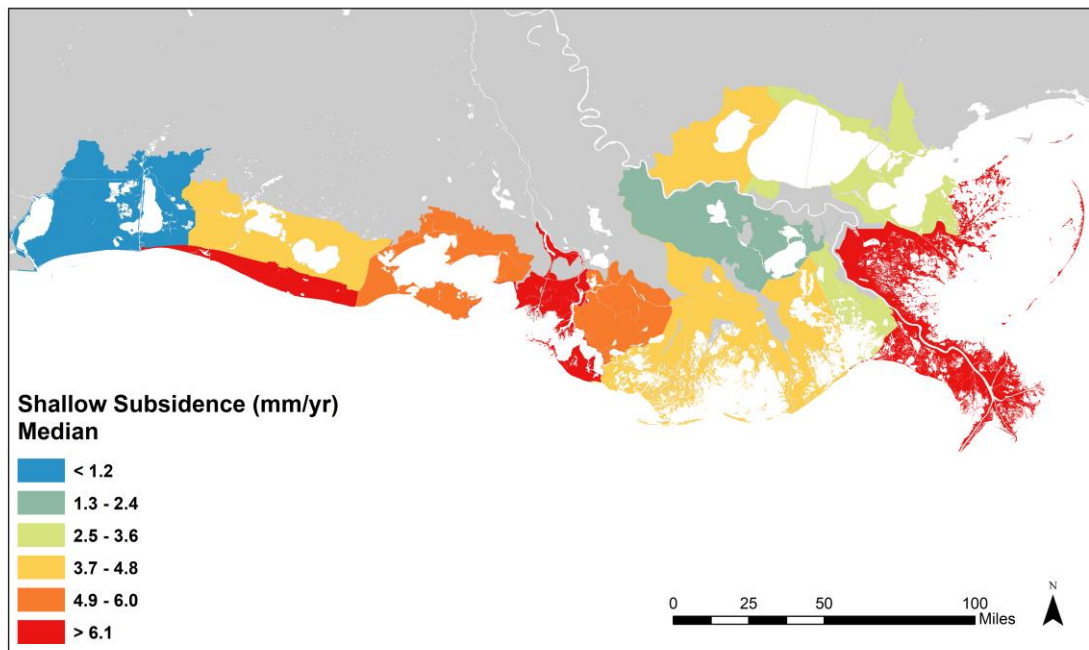


Figure 11. Median of shallow subsidence rate point data aggregated by ecoregion across coastal Louisiana. The map includes point data for shallow subsidence measured at 203 CRMS sites. Ecoregions with less than 2 points were aggregated into a neighboring ecoregion. Eastern Pontchartrain includes data from Biloxi Marsh SET data. Some smaller water bodies may not be represented on the map.

Certain areas along the coast are leveed, poldered, and/or impacted by forced drainage. These areas were omitted (extracted by mask and shown as grey in Figure 10 and Figure 11) from the SS layer, as extending SS measurements for wetlands is considered inappropriate for these areas (Figure 10 and Figure 11). For these masked areas, only DS values will be contributing to static subsidence rates applied for use in the ICM. This assumption means that unless processes such as consolidation, oxidation, and fluid withdrawal in urban/industrial areas are encompassed by the underlying DS data, they are not considered in the master plan analysis. As remote sensing becomes better suited to measurements in both urban and non-urban environments in the future, InSAR time series could be used to provide additional information on the areas excluded from the SS mask.

6.4 ASSUMPTIONS AND LIMITATIONS OF SHALLOW SUBSIDENCE APPROACH

As with DS, the development of a map of SS will always be subject to assumptions. Figure 10 and Figure 11 are designed to be used together with the map of DS to produce subsidence rates for use in master plan scale predictive modeling. They are not intended for use in design or operation of coastal restoration and protection projects that require site-specific information. The maps show broad spatial patterns generally representative of measured values for SS but may miss local variations.

The development of two maps to be applied in separate scenarios accommodates, to some extent, the uncertainty in SS rates. The first quartile and median aggregated SS estimates are both conservative relative to the range of observed rates. This is meant to account for the potential overlap in SS RSET measurements and DS benchmark measurements (Figure 5), especially in areas such as lower Terrebonne and Barataria basins.

Very little is known about the specific processes contributing to SS at any location or time period. Processes could include root zone collapse from reduced root production, increased decomposition of plant roots, loss of root volume, and compaction (Cahoon et al., 2020). The assumption being made here is that the set of processes contributing to SS during the 10+ years over which the RSET-MH data were collected will continue for the future period (50 years) of the master plan analysis. Sites with high interannual variability (i.e., sites with a very low coefficient of determination for either SEC or VA), as well as sites with limited amounts of data and/or shallow subsidence values 2 standard deviations outside of the mean were eliminated. This site omission reduced variability within ecoregions and may have excluded sites where the data were dominated by individual events; there is no basis for assuming that such variability or events would continue for decades into the future.

In addition, there are some processes that could result in shallow expansion (i.e., 'negative shallow subsidence'), such as the shrink-swell processes noted above. CRMS data showing net shallow expansion for the period of record were not eliminated from the analysis. Note that the first quartile value for the Sabine ecoregion (Table 4) is negative. Flotant marsh sites (i.e., where sites were understood to be frequently inundated and more responsive to water level fluctuations than subsurface processes) were omitted from this analysis, though they are still tracked in the ICM (Visser et al., 2017). However, the modeling assumes their surface elevation is not influenced by subsidence (DS or SS), and they are not subject to accretion. Thus, the omission of flotant areas from this data set does not limit the application of the SS rates for the 2023 Coastal Master Plan analysis.

7.0 SUMMARY

7.1 DEEP SUBSIDENCE PATTERNS

The patterns of DS shown in Figure 7 generally conform to established conceptual models of geologically controlled subsidence in Louisiana (e.g., Roberts et al., 1994; Kulp et al., 2002). Rates are generally greater in areas of greater Holocene sediment thickness (e.g., in the Bird's Foot Delta and over the incised valley on the Mississippi River) and lower in the Chenier Plain and to the north. In relation to recent measurements of subsidence (Table 2), there is some consistency for areas north of Lake Pontchartrain. As noted, few supplementary benchmarks were available in this region, so the DS rate is based on very limited data. Although specific fault movement is not considered in the approach used here, the DS rates are within the range of rates reported by Yaeger et al. (2012) and Shen et al. (2017). Compared to the analysis of 17 CORS stations by Karegar et al. (2016), the regional pattern is similar (lower rates to the west and north) but maximum rates presented in this report are higher. This is likely due to the larger number of stations used in this analysis (47), and the availability of data in areas of deep Holocene deposition.

The point subsidence estimates derived by Byrnes et al. (2019) and ACRE (2019) are used in the DS surface shown in Figure 6. Thus, patterns are similar, although differences in interpolation over a wider area lead to some differences, and coloration of interpolated maps can suggest greater differences than may be apparent in the actual surface. Indeed, ACRE (2019) notes uncertainty in some of the boundaries between subsidence zones they identify.

Limited availability of DS data in areas with differing geological histories (e.g., Chenier Plain and the North Shore of Lake Pontchartrain) has been supplemented with broad assumptions about the driving processes and estimates of their rates from other studies or expert evaluations. As noted above, a study of DS rates in Terrebonne Basin and west to Freshwater Bayou is underway, but results are not yet available.

7.2 SHALLOW SUBSIDENCE PATTERNS

SS patterns (Figure 10 and Figure 11) show areas of higher SS across both scenarios in the lower Mermentau basin, north of Atchafalaya Bay, and the Bird's Foot Delta. This is consistent with patterns identified by Jankowski et al. (2017), which is to be expected as the analysis used here is similar but uses an extended data set from CRMS. The extension of SS data from individual points in wetlands to the landscape scale leads to the issue of the types of coastal environments to which the data are applicable.

Much is still unknown about SS and it cannot be assumed that it occurs equally throughout the sediment column. Thus, prorating SS by depth (e.g., if SS is measured over the top 20 m and the bays

are 5 m deep, then apply SS to the bays but reduce by 25%) may not be reasonable. Within the context of the master plan analysis, if SS is indeed occurring beneath the coastal bays, then bay bottoms will be shallower than they should be in predicted future landscapes and may be more readily infilled by depositional processes. However, there are few areas of the coast where reliable and consistent bathymetric surveys are available to assess the impact, therefore separating that effect from changes in bathymetry due to erosion, deposition, etc., would be challenging. The effects on bay bed elevation may also be relatively small over a 50-year period (3 mm over 50 years = 15 cm), and may be within the error of bathymetry data used to initialize the models (Couvillion, 2017).

7.3 TOTAL SUBSIDENCE RATES

This report has focused on the independent development of maps for deep and shallow subsidence. They each apply to slightly different spatial domains and are driven by the available data and the types of environments to which they are considered best applied. For much of the coastal wetland landscape, the rates will be considered additive in the 2023 Coastal Master Plan analysis. The DS rates will apply in coastal bays and non-wetland areas. The TS rates will vary by scenario and area; composite maps are shown in Figure 12 and Figure 13. The DS rates will apply in coastal bays and non-wetland areas.

The maps of DS (Figure 7) and SS (Figure 10 and Figure 11) showed some consistent areas of high subsidence, and these are apparent in the TS surface (Figure 12 and Figure 13). The highest rates of TS are in the Bird's Foot Delta with slightly lower rates in central Terrebonne and near the Atchafalaya and Wax Lake Deltas. The lowest TS rates are in the western Chenier Plain and the North Shore of Lake Pontchartrain. These patterns are consistent across both the lower and higher scenario. Some of the areas with higher rates, especially central Terrebonne, are also areas where the CRMS site RSET rod is deeper than the interpolated foundation depth of CORS sites or secondary benchmarks (Figure 5). This may cause an overestimation of total subsidence, where subsidence for part of the substrate is included in both SS and DS measurements. In addition, some of the areas with low total subsidence on Figure 12 and Figure 13 are those where some part of the sediment column is not accounted for by the measurements (e.g., parts of the Chenier Plain).

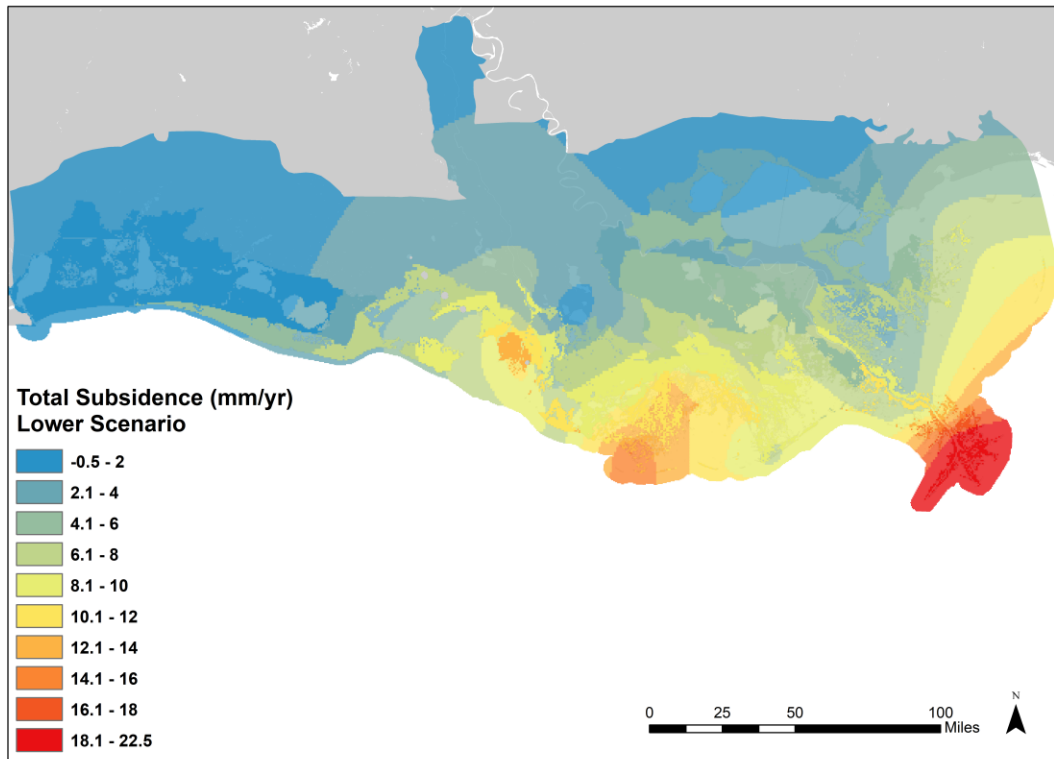


Figure 12. Coastwide map of total subsidence rates for the lower scenario.

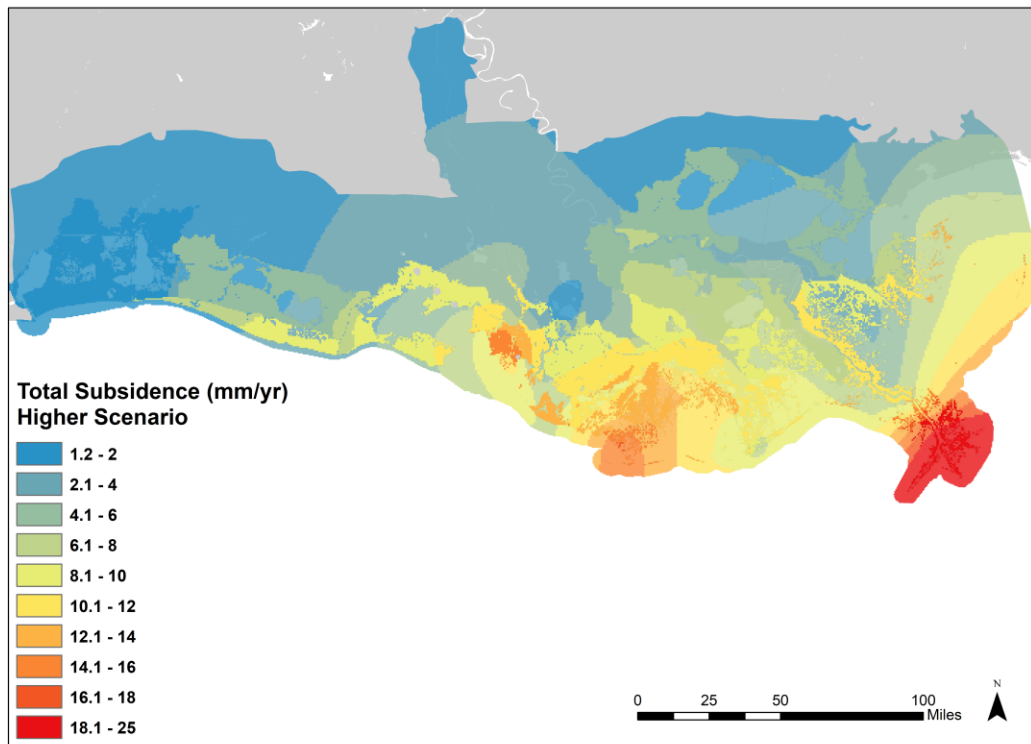


Figure 13. Coastwide map of total subsidence rates for the higher scenario.

The subsidence rates resulting from the analysis presented here will be applied for the duration of the 50 year simulations, i.e., rates will not change at a location over time. Thus, the role of periodic influences on subsidence, e.g., sudden collapse of the root zone (Chambers et al., 2019) or fault activation (Gagliano et al., 2003) will not be considered. Such processes are difficult to predict in time and space even with detailed local information, and will only be considered in the master plan analysis to the extent that they have contributed to measured SEC and VA.

Within the master plan modeling framework, it is possible to conduct analyses to characterize both ICM parametric uncertainty and ICM sensitivity to selected values for external drivers such as rates of subsidence. The total subsidence rates developed here can be used to compare how sensitive ICM land area outputs are to subsidence rates in relation to other uncertainties in land area calculations (e.g., model ‘error’ defined during the model validation process). It is also possible to evaluate spatial patterns of the sensitivity to subsidence rates, including which areas are predicted to be land under the lower and higher scenario that would be open water with different subsidence rates. The data analysis described in this report enables exploration of several aspects of uncertainty related to subsidence (e.g., other quartiles for SS foundation depth differences) and provides a platform for such assessments. Additional opportunities to evaluate uncertainty will be explored once the full results of

the ICM validation process are available.

As previously mentioned, the question of which rates to use to characterize subsidence across coastal Louisiana is a consequential consideration. Previous master planning efforts have considered the effects of subsidence on future environmental conditions and project outcomes using rates based on expert judgement. A comparison of 2012 and 2017 Coastal Master Plan subsidence ranges and the 2023 Coastal Master Plan subsidence rates by 2012 subsidence polygons (Figure 3) can be found in Appendix B, Table B3. As the TS rates shown in Figure 12 and Figure 13 vary across the subsidence subregions (Figure 3), direct comparison is difficult. However, for large areas of the coast, including the Cheniers, and the Breton and Pontchartrain sub-regions, the subsidence rates used previously are within the range of values to be used for the 2023 Coastal Master Plan analysis. For many of the impounded or poldered areas, where SS values are not applied, the total subsidence rates are lower than those previously applied (e.g., in the Golden Meadow and NOLA sub-regions). However, as the new TS rates will be applied as a continuous surface across the coast, local variations may be greater. The approach used for the 2023 Coastal Master Plan analysis is data-driven, which provides an additional level of transparency in the decision-making process.

8.0 REFERENCES

- Al Mukaimi, M. E., Dellapenna, T. M., & Williams, J. R. (2018). Enhanced land subsidence in Galveston Bay, Texas: Interaction between sediment accumulation rates and relative sea level rise. *Estuarine, Coastal and Shelf Science*, 207, 183–193. <https://doi.org/10.1016/j.ecss.2018.03.023>
- Applied Coastal Research and Engineering (ACRE) (2019). Determining Recent Subsidence Rates for Breton Sound and Eastern Pontchartrain Basins, Louisiana: Implications for Engineering and Design of Coastal Restoration Projects. Final Report prepared for Louisiana Coastal Protection and Restoration Authority. Contract 4400009020, Task 8, 58 p.
- Bekaert, D. S. P., C. E. Jones, K. An, M.-H. Huang (2018). Exploiting UAVSAR for a comprehensive analysis of subsidence in the Sacramento Delta. *Remote Sensing of Environment*, 220, 124-134. <https://doi.org/10.1016/j.rse.2018.10.023>
- Baustian, M., Reed, D., Visser J., Duke-Sylvester, S., Snedden, G., Wang, H., DeMarco, K., Foster-Martinez, M., Sharp L.A., McGinnis, T., and, Jarrell, E. Technical Report: ICM-Wetlands, Vegetation, and Soils Model Improvement Team. In Prep.
- Blum, M. D., & Roberts, H. H. (2012). The Mississippi delta region: past, present, and future. *Annual Review of Earth and Planetary Sciences*, 40, 655-683. <https://doi.org/10.1146/annurev-earth-042711-105248>
- Blum, M. D., Tomkin, J. H., Purcell, A., & Lancaster, R. R. (2008). Ups and downs of the Mississippi Delta. *Geology*, 36(9), 675-678. <https://doi.org/10.1130/G24728A.1>
- Byrnes, M. R., Hedderman, C., Hasen, M., Roberts, H., Khalil, S., & Underwood, S. G. (2015). Differential sediment consolidation associated with barrier beach restoration: Caminada Headland, South Louisiana. *The Proceedings of the Coastal Sediments 2015*. https://doi.org/10.1142/9789814689977_0192
- Byrnes, M. R., Britsch, L. D., Berlinghoff, J. L., Johnson, R., & Khalil, S. (2019). Recent subsidence rates for Barataria Basin, Louisiana. *Geo-Marine Letters* 39, 265-278. <https://doi.org/10.1007/s00367-019-00573-3>
- Cahoon, D. R., Reed, D. J., & Day Jr, J. W. (1995). Estimating shallow subsidence in microtidal salt marshes of the southeastern United States: Kaye and Barghoorn revisited. *Marine Geology*, 128(1-2), 1-9. [https://doi.org/10.1016/0025-3227\(95\)00087-F](https://doi.org/10.1016/0025-3227(95)00087-F)
- Cahoon, D. R., Lynch, J. C., & Knaus, R. M. (1996). Improved cryogenic coring device for sampling wetland soils. *Journal of Sedimentary Research*, 66(5), 1025-1027. <https://doi.org/10.2110/jsr.66.1025>

- Cahoon, D. R., Lynch, J. C., Hensel, P., Boumans, R., Perez, B. C., Segura, B., & Day Jr, J. W. (2002). High-precision measurements of wetland sediment elevation: I. Recent improvements to the sedimentation-erosion table. *Journal of Sedimentary Research*, 72(5), 730-733.
<https://doi.org/10.1306/020702720730>
- Cahoon D.R., Hensel P.F., Spencer T., Reed D.J., McKee K.L., Saintilan N. (2006). Coastal Wetland Vulnerability to Relative Sea-Level Rise: Wetland Elevation Trends and Process Controls. In: Verhoeven J.T.A., Beltman B., Bobbink R., Whingham D.F. (Eds.), pp. 271-292. *Wetlands and Natural Resource Management. Ecological Studies (Analysis and Synthesis)*, 190. Berlin Heidelberg: Springer-Verlag. https://doi.org/10.1007/978-3-540-33187-2_12
- Cahoon, D., Reed, D., Day, J., Lynch, J., Swales, A., & Lane, R. (2020). Applications and utility of the surface elevation table - marker horizon method for measuring wetland elevation and shallow soil subsidence-expansion. DISCUSSION/REPLY TO: Byrnes M, Britsch L, Berlinghoff J, Johnson R, Khalil S. 2019. Recent subsidence rates for Barataria Basin, Louisiana. *Geo-Marine Letters*, 39, 265-278. *Geo-Marine Letters*, 40, 809-815.
<https://doi.org/10.1007/s00367-020-00656-6>
- Chambers, L. G., H. E. Steinmuller, and J. L. Breithaupt. (2019). Toward a mechanistic understanding of “peat collapse” and its potential contribution to coastal wetland loss. *Ecology*, 100(7).
<https://doi.org/10.1002/ecy.2720>
- Childs, C. (2004). Interpolating Surfaces in ArcGIS Spatial Analyst. *ArcUser*, July-September, 32-35.
- Coastal Protection and Restoration Authority of Louisiana. (2012). Louisiana’s Comprehensive Master Plan for a Sustainable Coast. Coastal Protection and Restoration Authority of Louisiana, Baton Rouge, LA.
- Coastal Protection and Restoration Authority of Louisiana. (2017). Louisiana’s Comprehensive Master Plan for a Sustainable Coast. Coastal Protection and Restoration Authority of Louisiana, Baton Rouge, LA.
- Cobell, Z., Zhao, H., Roberts, H. J., Clark, F. R., & Zou, S. (2013). Surge and Wave Modeling for the Louisiana 2012 Coastal Master Plan. *Journal of Coastal Research*, 67(SI), 88–108.
https://doi.org/10.2112/SI_67_7
- Couvillion, B. (2017). 2017 Coastal Master Plan Modeling: Attachment C3-27: Landscape Data. Version Final. (pp. 1-84). Baton Rouge, Louisiana: Coastal Protection and Restoration Authority.
- Fischbach, J.R., Johnson, D.R., Kuhn, K., Pollard, M., Stelzner, C., Costello, R., Molina, E., Sanchez, R., Syme, J., Roberts, H., & Cobell, Z. (2017). 2017 Coastal Master Plan Modeling: Attachment C3- 25: Storm Surge and Risk Assessment. Version Final. (pp. 1-219). Baton Rouge, Louisiana: Coastal Protection and Restoration Authority.

- Flocks, J. Smith, and S.J. Williams, (2009). Review of the geologic history of the Pontchartrain Basin, northern Gulf of Mexico. *Journal Coastal Research*, 10054, 12-22.
<https://doi.org/10.2112/SI54-013.1>
- Frederick, B. C., Blum, M., Fillon, R., & Roberts, H. (2019). Resolving the contributing factors to Mississippi Delta subsidence: Past and Present. *Basin Research*, 31(1), 171–190.
<https://doi.org/10.1111/bre.12314>
- Gagliano, S. M., Iii, E. B. K., Wicker, K. M., Wiltenmuth, K. S., & Sabate, R. W. (2003). Neo-Tectonic Framework of Southeast Louisiana and Applications to Coastal Restoration. *Gulf Coast Association of Geological Societies Transactions*, 53, 262–276.
- Geoghegan, C. E., Breidenbach, S. E., Lokken, D. R., Fancher, K. L., & Hensel, P. F. (2009). Procedures for Connecting SET Bench Marks to the NSRS. NOAA Technical Report NOS NGS-61. National Geodetic Survey, Silver Spring, MD.
- González, J. L., & Tornqvist, T. E. (2006). Coastal Louisiana in crisis: Subsidence or sea level rise?. *Eos, Transactions American Geophysical Union*, 87(45), 493-498.
<https://doi.org/10.1029/2006EO450001>
- Grall, C., Steckler, M. S., Pickering, J. L., Goodbred, S., Sincavage, R., Paola, C., Akhter, S. H., & Spiess, V. (2018). A base-level stratigraphic approach to determining Holocene subsidence of the Ganges–Meghna–Brahmaputra Delta plain. *Earth and Planetary Science Letters*, 499, 23–36. <https://doi.org/10.1016/j.epsl.2018.07.008>
- Groves, D. G., & Lempert, R. J. (2007). A new analytic method for finding policy-relevant scenarios. *Global Environmental Change*, 17(1), 73-85.
<https://doi.org/10.1016/j.gloenvcha.2006.11.006>
- Harris, J. B., Joyner, T. A., Rohli, R. V., Friedland, C. J., & Tollefson, W. C. (2020). It's all Downhill from Here: A forecast of subsidence rates in the lower Mississippi River industrial corridor. *Applied Geography*, 114, 102123. <https://doi.org/10.1016/j.apgeog.2019.102123>
- Higgins, S. A. (2016). Review: Advances in delta-subsidence research using satellite methods. *Hydrogeology Journal*, 24(3), 587–600. <https://doi.org/10.1007/s10040-015-1330-6>
- Jafari, N. H., Harris, B. D., & Stark, T. D. (2018). Long-term subsidence of beach nourishment and dune restoration in Caminada headlands, coastal Louisiana. *Coastal Engineering Proceedings*, 1(36). <https://doi.org/10.9753/icce.v36.risk.66>
- Jankowski, K. L., Törnqvist, T. E., & Fernandes, A. M. (2017). Vulnerability of Louisiana's coastal wetlands to present-day rates of relative sea-level rise. *Nature Communications*, 8(1), 1–7.
<https://doi.org/10.1038/ncomms14792>
- Jones, C. E., An, K., Blom, R. G., Kent, J. D., Ivins, E. R., & Bekaert, D. (2016). Anthropogenic and

- geologic influences on subsidence in the vicinity of New Orleans, Louisiana. *Journal of Geophysical Research: Solid Earth*, 121(5), 3867-3887.
<https://doi.org/10.1002/2015JB012636>
- Karegar, M. A., Dixon, T. H., & Engelhart, S. E. (2016). Subsidence along the Atlantic Coast of North America: Insights from GPS and late Holocene relative sea level data. *Geophysical Research Letters*, 43(7), 3126-3133. <https://doi.org/10.1002/2016GL068015>
- Keogh, M. E., & Törnqvist, T. E. (2019). Measuring rates of present-day relative sea-level rise in low-elevation coastal zones: a critical evaluation. *Ocean Science*, 15(1), 61-73.
<https://doi.org/10.5194/os-15-61-2019>
- Kirwan, M. L. & Guntenspergen, G. R. (2012). Feedbacks between inundation, root production, and shoot growth in a rapidly submerging brackish marsh. *Journal of Ecology*, 100(3), 764–770.
<https://doi.org/10.1111/j.1365-2745.2012.01957.x>
- Kulp, M., Howell, P., Adiau, S., Penland, S., Kindinger, J., & Williams, S. J. (2002). Latest Quaternary stratigraphic framework of the Mississippi River delta region. *Gulf Coast Association of Geological Societies Transactions*, 52, 573-582.
- Kulp, S. A., & Strauss, B. H. (2019). New elevation data triple estimates of global vulnerability to sea-level rise and coastal flooding. *Nature Communications*, 10(1), 1–12.
<https://doi.org/10.1038/s41467-019-12808-z>
- Lane, R. R., Reed, D. J., Day, J. W., Kemp, G. P., McDade, E. C., & Rudolf, W. B. (2020). Elevation and accretion dynamics at historical plots in the Biloxi Marshes, Mississippi Delta. *Estuarine, Coastal and Shelf Science*, 245, 106970. <https://doi.org/10.1016/j.ecss.2020.106970>
- Mahmoud, M., Liu, Y., Hartmann, H., Stewart, S., Wagener, T., Semmens, D., Stewart, R., ... Winter, L. (2009). A formal framework for scenario development in support of environmental decision-making. *Environmental Modelling & Software*, 24(7), 798-808.
<https://doi.org/10.1016/j.envsoft.2008.11.010>
- Meckel, T. A., ten Brink, U. S., & Williams, S. J. (2006). Current subsidence rates due to compaction of Holocene sediments in southern Louisiana. *Geophysical Research Letters*, 33(11).
<https://doi.org/10.1029/2006GL026300>
- Meselhe, E., White, E. D., and Reed, D. J., (2017a). 2017 Coastal Master Plan: Appendix C: Modeling Chapter 2 – Future Scenarios. Version Final. (p. 32). Baton Rouge, Louisiana: Coastal Protection and Restoration Authority.
- Meselhe, E.M, White, E.D., and Wang, Y. (2017b). 2017 Coastal Master Plan: Attachment C3-24: Integrated Compartment Model Uncertainty Analysis. (pp. 1-68). Baton Rouge, Louisiana: Coastal Protection and Restoration Authority.

- Minderhoud, P. S. J., Coumou, L., Erban, L. E., Middelkoop, H., Stouthamer, E., & Addink, E. A. (2018). The relation between land use and subsidence in the Vietnamese Mekong delta. *Science of The Total Environment*, 634, 715–726. <https://doi.org/10.1016/j.scitotenv.2018.03.372>
- Morris, J. T., Sundareshwar, P. V., Nietch, C. T., Kjerfve, B. & Cahoon, D. R. (2002). Responses of coastal wetlands to rising sea level. *Ecology*, 83, 2869–2877. [https://doi.org/10.1890/0012-9658\(2002\)083\[2869:ROCWTR\]2.0.CO;2](https://doi.org/10.1890/0012-9658(2002)083[2869:ROCWTR]2.0.CO;2)
- Morton, R. A., & Bernier, J. C. (2010). Recent subsidence-rate reductions in the Mississippi Delta and their geological implications. *Journal of Coastal Research*, (263), 555-561. <https://doi.org/10.2112/JCOASTRES-D-09-00014R1.1>
- Murray, A.S. (2020). Water exchange in near-surface marsh strata of Barataria Basin, Louisiana and the implications for subsidence (Master's thesis, Tulane University School of Engineering and Science, New Orleans, Louisiana). Retrieved from <https://digitalibrary.tulane.edu/islandora/object/tulane%3A120511>
- Peyronnin, N., Green, M., Richards, C. P., Owens, A., Reed, D., Chamberlain, J., Groves, D. G., Rhinehart, W. K., & Belhadjali, K. (2013). Louisiana's 2012 Coastal Master Plan: Overview of a Science-Based and Publicly Informed Decision-Making Process. *Journal of Coastal Research*, 67(SI), 1–15. https://doi.org/10.2112/SI_67_1.1
- Qu, F., Lu, Z., Kim, J.-W., & Zheng, W. (2019). Identify and Monitor Growth Faulting Using InSAR over Northern Greater Houston, Texas, USA. *Remote Sensing*, 11(12), 1498. <https://doi.org/10.3390/rs11121498>
- Reed, D., & Yuill, B. (2017). 2017 Coastal Master Plan: Attachment C2-2: Subsidence. Version Final. (p. 15). Baton Rouge, Louisiana: Coastal Protection and Restoration Authority.
- Roberts, H.H., 1985. A study of sedimentation and subsidence in the south-central coastal plain of Louisiana. Final report to the U. S. Army Corps of Engineers, New Orleans District, New Orleans, Louisiana, 53 p.
- Roberts, H. H., Bailey, A., & Kuecher, G. J. (1994). Subsidence in the Mississippi River Delta— Important Influences of Valley Filling by Cyclic Deposition, Primary Consolidation Phenomena, and Early Diagenesis, 44, 619-629.
- Sella, G. F., Stein, S., Dixon, T. H., Craymer, M., James, T. S., Mazzotti, S., & Dokka, R. K. (2007). Observation of glacial isostatic adjustment in “stable” North America with GPS. *Geophysical Research Letters*, 34(2). <https://doi.org/10.1029/2006GL027081>
- Shen, Z., Dawers, N. H., Törnqvist, T. E., Gasparini, N. M., Hijma, M. P., & Mauz, B. (2017). Mechanisms of Late Quaternary fault throw-rate variability along the north central Gulf of Mexico coast: Implications for coastal subsidence. *Basin Research*, 29(5), 557-570. <https://doi.org/10.1111/bre.12184>

- Swales, A., Denys, P., Pickett, V. I., & Lovelock, C. E. (2016). Evaluating deep subsidence in a rapidly-accreting mangrove forest using GPS monitoring of surface-elevation benchmarks and sedimentary records. *Marine Geology*, 380, 205-218. <https://doi.org/10.1016/j.margeo.2016.04.015>
- Syvitski, J. P. M., Kettner, A. J., Overeem, I., Hutton, E. W. H., Hannon, M. T., Brakenridge, G. R., Day, J., Vörösmarty, C., Saito, Y., Giosan, L., & Nicholls, R. J. (2009). Sinking deltas due to human activities. *Nature Geoscience*, 2(10), 681–686. <https://doi.org/10.1038/ngeo629>
- Takagi, H., Thao, N. D., & Anh, L. T. (2016). Sea-Level Rise and Land Subsidence: Impacts on Flood Projections for the Mekong Delta's Largest City. *Sustainability*, 8(9), 959. <https://doi.org/10.3390/su8090959>
- Visser, J. M., Duke-Sylvester S. M., Shaffer, G. P., Hester, M. W., Couvillion, B., Broussard, W. P. III, Willis, J.M., and Beck H. (2017). 2017 Coastal Master Plan: Attachment C3-5: Vegetation. Version Final. (pp. 1-128). Baton Rouge, Louisiana: Coastal Protection and Restoration Authority.
- White, E. D., Meselhe, E., McCorquodale, A., Couvillion, B., Dong, Z., Duke-Sylvester, S. M., & Wang, Y. (2017). 2017 Coastal Master Plan: Attachment C3-22: Integrated Compartment Model (ICM) Development. Version Final (pp. 1-49). Baton Rouge, Louisiana: Coastal Protection and Restoration Authority.
- White, E.D., Meselhe, E, McCorquodale, A, Couvillion, B, Dong, Z, Duke-Sylvester, S.M., & Wang, Y. (2017). 2017 Coastal Master Plan: Attachment C2-22: Integrated Compartment Model (ICM) Development. Version Final. (pp. 1-49). Baton Rouge, Louisiana: Coastal Protection and Restoration Authority.
- White, E. D., Reed, D. J., & Meselhe, E. A. (2019). Modeled Sediment Availability, Deposition, and Decadal Land Change in Coastal Louisiana Marshes under Future Relative Sea Level Rise Scenarios. *Wetlands*, 39, 1233-1248. <https://doi.org/10.1007/s13157-019-01151-0>
- Wolstencroft, M., Shen, Z., Törnqvist, T. E., Milne, G. A., & Kulp, M. (2014). Understanding subsidence in the Mississippi Delta region due to sediment, ice, and ocean loading: Insights from geophysical modeling. *Journal of Geophysical Research: Solid Earth*, 119(4), 3838-3856. <https://doi.org/10.1002/2013JB010928>
- Yeager, K. M., Brunner, C. A., Kulp, M. A., Fischer, D., Feagin, R. A., Schindler, K. J., ... & Bera, G. (2012). Significance of active growth faulting on marsh accretion processes in the lower Pearl River, Louisiana. *Geomorphology*, 153, 127-143. <https://doi.org/10.1016/j.geomorph.2012.02.018>

Yu, S. Y., Törnqvist, T. E., & Hu, P. (2012). Quantifying Holocene lithospheric subsidence rates underneath the Mississippi Delta. *Earth and Planetary Science Letters*, 331, 21-30. <https://doi.org/10.1016/j.epsl.2012.02.021>

Yuill, B., Lavoie, D., & Reed, D. J. (2009). Understanding Subsidence Processes in Coastal Louisiana. *Journal of Coastal Research*, 2009(10054), 23–36. <https://doi.org/10.2112/SI54-012.1>

9.0 APPENDICES

APPENDIX A: Common Approaches to Subsidence Measurement 54
APPENDIX B: Supplemental Information for Subsidence Map Development..... 57

APPENDIX A: COMMON APPROACHES TO SUBSIDENCE MEASUREMENT

Table A1. Several approaches to measuring rates of subsidence are described. Each method is capable of providing measurements on a particular spatial and temporal scale and its applicability to calculation of DS, SS or TS indicated.

TECHNIQUE	DESCRIPTION	SPATIAL SCALE	TEMPORAL SCALE	SS/ DS/ TS
Re-Survey of Benchmarks	A TIME SERIES OF RE-LEVELING SURVEYS DOCUMENTING THE VERTICAL POSITION OF MONUMENTED BENCHMARKS IN RESPECT TO A STABLE VERTICAL DATUM	RE-LEVELING SURVEYS MEASURE POINT SUBSIDENCE.	THE REOCCURRENCE INTERVAL OF THE SURVEYS DETERMINES THE TEMPORAL SCALE OF THE DERIVED RATE.	DS
Continuously Operating Reference Stations (CORS)	A GPS DESIGNED TO MEASURE AND RECORD A CONTINUOUS RECORD OF ITS THREE-DIMENSIONAL GPS POSITION AT A FIXED LOCATION	POINT MEASUREMENT OF SUBSIDENCE AT A FIXED LOCATION. CORS NETWORKS CAN ESTIMATE FIELDS OF SUBSIDENCE AT A REGIONAL SCALE.	CORS DATASETS CONSIST OF NEAR CONTINUOUS MEASUREMENTS AND DURATION DEPENDING ON LENGTH OF DEPLOYMENT.	DS
Interferometric synthetic aperture radar (InSAR)	A REMOTE SENSING TECHNIQUE USED TO MEASURE DISPLACEMENT FROM A TIME SERIES OF COHERENT MICROWAVE RADAR BACKSCATTERED AMPLITUDE AND PHASE DATASETS.	MAPS OF SUBSIDENCE BASED ON REPEAT MEASUREMENTS THAT GIVE CHANGE SURFACE POSITION ALONG THE LINE-OF-SIGHT DIRECTION.	COMPUTES SUBSIDENCE BASED ON CUMULATIVE SURFACE DISPLACEMENT BETWEEN TWO OR MORE ACQUISITIONS MADE AT DIFFERENT TIMES.	TS

TECHNIQUE	DESCRIPTION	SPATIAL SCALE	TEMPORAL SCALE	SS/ DS/ TS
Sediment elevation tables (SETs)	STATIONARY INSTRUMENTS MOUNTED ON PERMANENT RODS IN WETLANDS TO MEASURE SURFACE ELEVATION CHANGE (RELATIVE TO THE DEPTH OF THE ROD). WHEN COMBINED WITH MEASUREMENTS OF SURFACE VERTICAL ACCRETION SETS CAN MEASURE SHALLOW SUBSIDENCE	POINT MEASUREMENTS OF ELEVATION CHANGE AND SHALLOW SUBSIDENCE. SET NETWORKS MAY PRODUCE SUBSIDENCE VALUES EXTRAPOLATED TO THE LOCAL MARSH LEVEL.	COMPUTES ELEVATION CHANGE OR SHALLOW SUBSIDENCE BETWEEN TWO SEPARATE MEASUREMENTS IN TIME. TRENDS CAN BE FIT TO A TIME SERIES OF MEASUREMENTS.	SS
Chrono-stratigraphy	STRATA (USUALLY PEATS OR SANDS) ARE ASSUMED TO HAVE FORMED AT NEAR CONTEMPORANEOUS SEA LEVEL. KNOWLEDGE OF THE ELEVATION OF HISTORICAL SEA LEVELS IN RELATION TO THE AGE OF THE STRATA CAN THEN BE USED TO DETERMINE THE INITIAL ELEVATION OF THE STRATA AT THE TIME OF ITS FORMATION. DATING TECHNIQUE VARIES BY SEDIMENT TYPE.	POINT MEASUREMENTS (USUALLY TAKEN AS SEDIMENT CORES) OFTEN COMBINED WITH OTHER NEARBY MEASUREMENTS TO EXTRAPOLATE LOCAL AREAS OF SUBSIDENCE IF THE UNDERLYING GEOLOGY IS KNOWN.	PRODUCE MEAN RATES OF SUBSIDENCE CONSTRAINED BY THE PERIOD IN TIME FOR WHICH DATEABLE SEDIMENT IS AVAILABLE AND BY THE ASSUMPTIONS OF THE DATING TECHNIQUES (E.G., CS-137, C-14, OSL).	DS

TECHNIQUE	DESCRIPTION	SPATIAL SCALE	TEMPORAL SCALE	SS/ DS/ TS
Extensometers	STATIONARY INSTRUMENT CONSISTING OF A VERTICAL SHAFT ENCASED WITH A METAL TUBE. A ROD OR WIRE PASSES THROUGH THE TUBE AND IS ANCHORED AT THE BASE OF THE WELL. A DEVICE CALCULATES THE DISTANCE FROM THE BOTTOM OF THE ROD OR WIRE TO THE TOPOGRAPHICAL SURFACE ON WHICH IT RESTS. AS SUBSIDENCE OCCURS, THE LENGTH OF THE ROD OR WIRE BETWEEN THE BOTTOM OF THE WELL AND THE MEASUREMENT DEVICE AT THE SURFACE BECOMES SMALLER.	POINT BASED MEASUREMENTS OF SUBSIDENCE	MEASURE NEAR CONTINUOUS SUBSIDENCE DURING THE PERIOD OF INSTRUMENTATION/LENGTH OF DEPLOYMENT.	SS/DS
Fault offset measurements	THE VERTICAL DISPLACEMENT BETWEEN STRATA ON EITHER SIDE OF A FAULT. THE RELATIVE VERTICAL POSITION OF OFFSET SEDIMENTARY FACIES IS USED TO MEASURE THROW AND DATING OF THE FACIES ENABLES CALCULATION OF MEAN THROW RATES.	MEASUREMENTS OF SUBSIDENCE ASSOCIATED WITH INDIVIDUAL FAULTS	PRODUCE MEAN RATES OF FAULT THROW CONSTRAINED BY THE PERIOD IN TIME FOR WHICH DATEABLE SEDIMENT IS AVAILABLE AND BY THE ASSUMPTIONS OF THE DATING TECHNIQUES.	DS

APPENDIX B: SUPPLEMENTAL INFORMATION FOR SUBSIDENCE MAP DEVELOPMENT

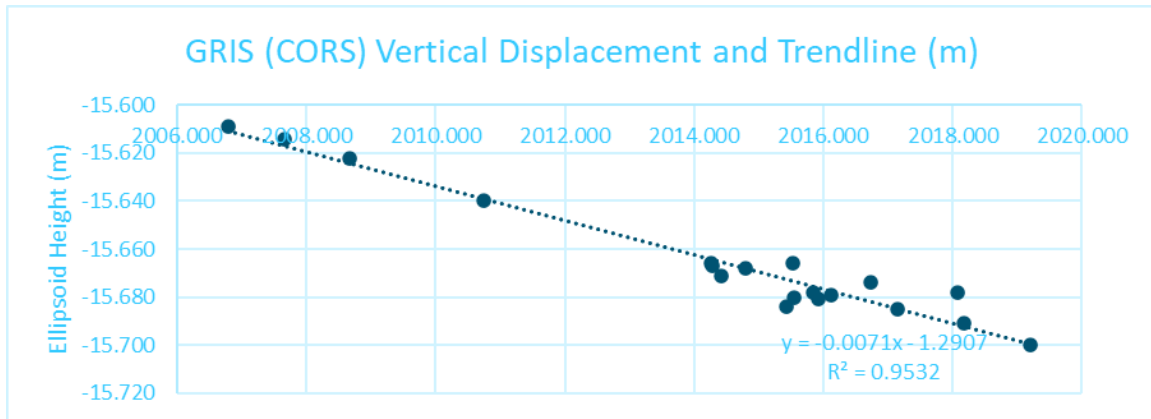


Figure B1. Sample calculations of vertical displacement at a CORS site, in this case at the GRIS site. Years along the X-axis are measured in decimal years. The subsidence rate at this site is the slope of the simple linear regression line (-0.0071 m/yr).

Table B1. All primary and secondary benchmark stations (CORS/NGS) from Byrnes et al. (2019) and ACRE (2019), as well as supplementary data compiled by CPRA and used in the calculation of DS. The "Benchmark Type" column indicates if data was obtained from a CORS station or secondary benchmark. The "Analysis" column indicates which group performed benchmark analysis. The R² column (coefficient of determination) provide an indication of uncertainty for the rates; missing values indicate there were only two observations for that station and a trendline could not be calculated. Stations highlighted in yellow were omitted. Three sites were omitted: MARY, SBCH, and G365. Sites were omitted because 1 cm or less of vertical change was recorded at each location (elevation measurements were made to an accuracy of >1 cm).

STATION	BASIN	BENCHMARK TYPE	SOURCE	FOUNDATION DEPTH (M)	YRS	DS RATE (MM/YR)	R2
Mary (CORS)	BE	CORS	BYRNES		4.95	1.3	0.51
SBCH (CORS)	BE	CORS	BYRNES	27	3.65	4.9	0.88
CRMS BS SM 01	BE	CRMS/NGS	BYRNES	12.2	7.87	3.2	
CRMS BS SM 02	BE	CRMS/NGS	BYRNES	10.97	12.68	2.5	0.99
CRMS BS SM 03	BE	CRMS/NGS	BYRNES	12.19	12.68	4.2	0.99
CRMS BS SM 04	BE	CRMS/NGS	BYRNES	12.19	12.68	4.1	0.88
CRMS BS SM 05	BE	CRMS/NGS	BYRNES	10.97	12.68	3.4	0.83
CRMS PO SM 05	BE	CRMS/NGS	BYRNES		4.81	5.4	
D194	BE	CRMS/NGS	BYRNES	36.58	3.89	3.9	
E3146	BE	CRMS/NGS	BYRNES	1	9.89	2.3	0.92
PIKE RESET	BE	CRMS/NGS	BYRNES		9.89	2.1	0.91
R194	BE	CRMS/NGS	BYRNES	29.26	3.89	3.9	
REGGIO2	BE	CRMS/NGS	BYRNES	20.73	13.64	2	0.57
BVHS (CORS)	BA	CORS	ACRE	BUILDING	15.01	5.2	0.94
GRIS (CORS)	BA	CORS	ACRE	BUILDING	11.30	7.1	0.96

STATION	BASIN	BENCHMARK TYPE	SOURCE	FOUNDATION DEPTH (M)	YRS	DS RATE (MM/YR)	R2
LWES (CORS)	BA	CORS	ACRE	BUILDING	8.65	3.2	0.41
ENG5 (CORS)	BA	CORS	ACRE	TOWER - 3	8.23	2.5	0.66
AWES (CORS)	BA	CORS	ACRE	BUILDING	7.65	2	0.79
CMS-BM-01	BA	CRMS/NGS	ACRE	1	5.20	5.4	0.96
BA01 SM 03	BA	CRMS/NGS	ACRE	15.85	14.97	4.8	0.99
BA01 SM 05	BA	CRMS/NGS	ACRE	15.85	15.01	4.3	0.99
BA02 SM 01	BA	CRMS/NGS	ACRE	19.51	15.01	5.2	0.82
BA02 SM 02	BA	CRMS/NGS	ACRE	15.85	14.97	5.4	0.93
BA03C SM 02	BA	CRMS/NGS	ACRE	14.63	15.01	5.1	0.99
BA15 SM 01	BA	CRMS/NGS	ACRE	14.63	11.34	4.6	
BA23 SM 02	BA	CRMS/NGS	ACRE		15.01	5.8	0.99
BA34 SM 04	BA	CRMS/NGS	ACRE	14.63	7.66	4.4	
BAFS SM 03H	BA	CRMS/NGS	ACRE	15.85	15.03	4.5	0.93
BA-SCOFIELD 2	BA	CRMS/NGS	ACRE	20.73	9.49	6.1	
EMPIRE AZ MK 2	BA	CRMS/NGS	ACRE	2.00	12.35	4.7	0.99
G365	BA	CRMS/NGS	ACRE	32.92	12.36	0.7	0.09
H359	BA	CRMS/NGS	ACRE	24.38	13.92	5.9	0.98
TE23 SM 01	BA	CRMS/NGS	ACRE	29.27	9.82	5.7	0.88
CRMSTE-SM-05	TE	CRMS/NGS	CPRA	24.38	7.25	9.4	

STATION	BASIN	BENCHMARK TYPE	SOURCE	FOUNDATION DEPTH (M)	YRS	DS RATE (MM/YR)	R2
CRMS TE SM19	TE	CRMS/NGS	CPRA	23.16	6.89	9.0	
CRMSTE SM 17	TE	CRMS/NGS	CPRA		7.25	8.0	
TE32-SM-04	TE	CRMS/NGS	CPRA	18.29	10.96	9.5	
CRMSTE-SM-06	TE	CRMS/NGS	CPRA	12.19	7.25	12.1	
MR09 SM 11	MR	CRMS/NGS	CPRA	22.71	11.24	17.7	
CRMSPO SM 30	PO	CRMS/NGS	CPRA	26.82	4.82	0.4	
PO29 SM 03	PO	CRMS/NGS	CPRA	15.85	10.51	1.2	
HOUM	TE	CORS	CPRA		15	4.3	
TE22-SM-01	TE	CRMS/NGS	CPRA	24.38	10.42	6.0	
CRMSAT-SM-04	AT	CRMS/NGS	CPRA	20.73	6.83	0.4	
AT03-SM-01	AT	CRMS/NGS	CPRA	19.51	10.5	3.9	
AT04-SM-01	AT	CRMS/NGS	CPRA		10.50	8.8	
FSHS	AT	CORS	CPRA		8	3.9	
ME16 SM 10	ME	CRMS/NGS	CPRA	12.19	6	1.7	
CALC	CS	CORS	CPRA		5.00	0.8	
CRMSCS-SM-08	CS	CRMS/NGS	CPRA	14.63	6.78	0.1	

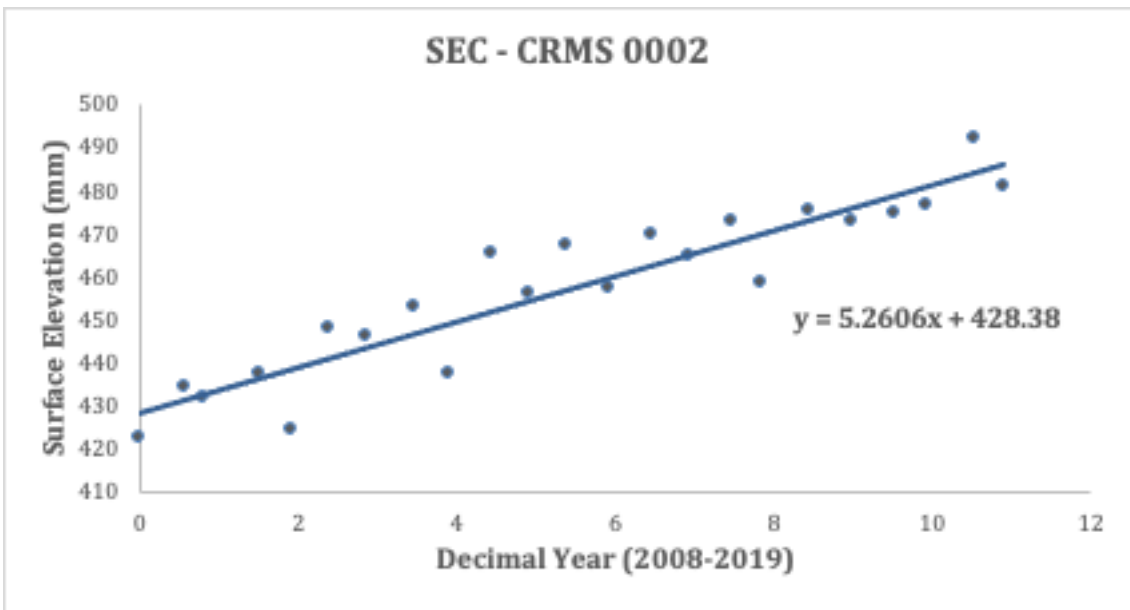
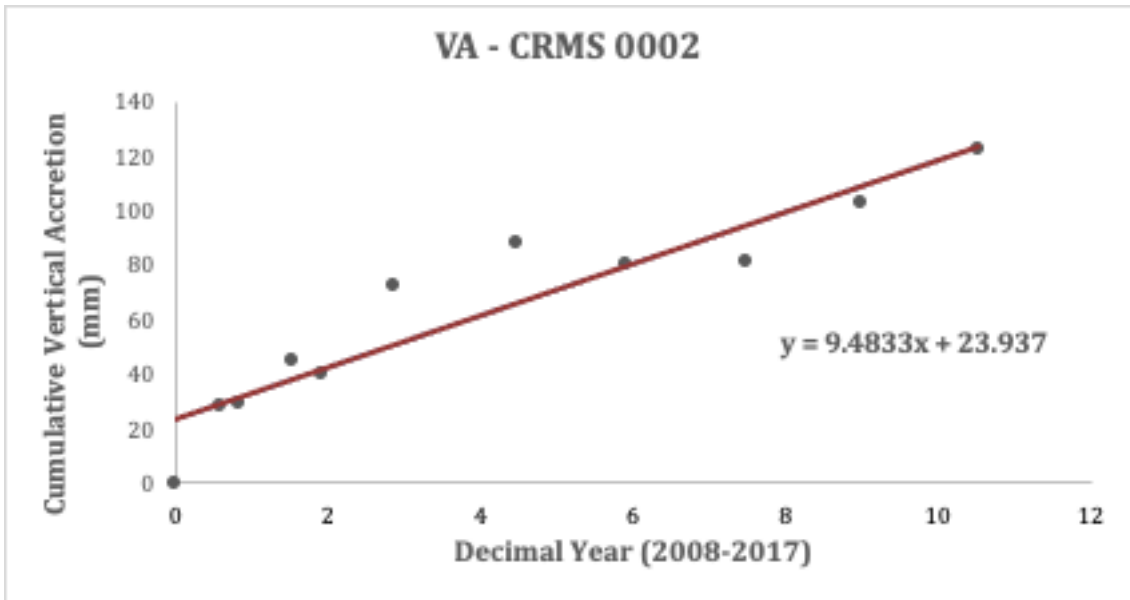


Figure B2. Vertical accretion (top) and surface elevation (bottom) data graphed as time series data. A vertical accretion rate (VA) was determined from the slope of the linear regression through all sample points. For CRMS0002, VA is 9.48 mm/yr and SEC is 5.26 mm/yr.

Table B2. Shallow subsidence rates (Figure 8), surface elevation change (Appendix B, Figure B3), and vertical accretion rates (Appendix B, Figure B4) by CRMS site.

SITE ID	SEC RATE (MM/YR)	SEC # POINTS	VA RATE (MM/YR)	VA # POINTS	SS RATE (MM/YR)
CRMS 0002	5.26	23	9.48	11	4.22
CRMS 0003	2.31	23	20.05	11	17.74
CRMS 0006	4.28	23	6.35	11	2.07
CRMS 0030	4.15	25	16.52	13	12.37
CRMS 0035	5.56	18	6.77	8	1.21
CRMS 0038	6.20	21	6.71	9	0.51
CRMS 0046	8.77	23	13.64	11	4.87
CRMS 0047	2.14	13	4.85	10	2.71
CRMS 0056	16.67	9	10.02	7	-6.64
CRMS 0061	4.05	13	7.30	11	3.24
CRMS 0086	2.46	21	5.61	9	3.15
CRMS 0097	3.94	20	8.56	8	4.62
CRMS 0103	7.88	21	9.62	9	1.74
CRMS 0108	7.57	21	7.00	9	-0.58
CRMS 0117	-6.66	21	9.47	8	16.13
CRMS 0118	9.58	21	16.13	9	6.55
CRMS 0129	4.66	23	6.09	6	1.43
CRMS 0131	-5.16	21	4.94	11	10.10
CRMS 0139	11.68	23	18.41	10	6.73
CRMS 0146	6.08	23	12.84	9	6.75
CRMS 0147	5.18	25	8.03	13	2.85
CRMS 0148	5.21	23	5.72	11	0.51
CRMS 0156	30.43	24	39.25	11	8.82
CRMS 0159	10.73	24	15.48	11	4.75
CRMS 0161	11.45	19	18.73	9	7.28
CRMS 0163	7.70	25	13.34	12	5.64
CRMS 0164	9.44	26	11.90	14	2.46

SITE ID	SEC RATE (MM/YR)	SEC # POINTS	VA RATE (MM/YR)	VA # POINTS	SS RATE (MM/YR)
CRMS 0171	9.44	25	16.33	8	6.90
CRMS 0172	7.14	24	16.36	7	9.23
CRMS 0173	10.25	25	6.91	13	-3.34
CRMS 0175	8.62	26	7.10	9	-1.52
CRMS 0179	6.63	22	20.96	11	14.33
CRMS 0181	13.93	24	17.84	6	3.91
CRMS 0194	3.50	21	11.70	7	8.20
CRMS 0197	3.15	21	5.61	9	2.46
CRMS 0209	8.47	25	9.68	13	1.21
CRMS 0217	7.10	21	7.82	9	0.72
CRMS 0220	3.70	24	9.88	10	6.18
CRMS 0224	4.32	25	3.66	12	-0.65
CRMS 0225	12.24	26	10.89	11	-1.35
CRMS 0226	8.29	25	10.27	13	1.99
CRMS 0232	7.84	26	11.28	14	3.44
CRMS 0237	22.52	26	25.94	9	3.42
CRMS 0248	7.02	24	8.72	12	1.70
CRMS 0251	5.69	25	10.36	13	4.67
CRMS 0253	6.24	26	20.70	11	14.46
CRMS 0260	10.04	23	15.28	11	5.24
CRMS 0261	6.63	24	10.47	12	3.85
CRMS 0263	-4.23	22	8.40	9	12.63
CRMS 0272	10.99	23	17.21	11	6.22
CRMS 0276	9.49	22	10.80	10	1.31
CRMS 0292	9.06	26	14.26	12	5.20
CRMS 0293	5.09	26	6.16	14	1.08
CRMS 0303	3.37	26	7.70	14	4.33
CRMS 0305	10.51	26	13.68	13	3.17
CRMS 0307	7.98	25	15.60	13	7.62
CRMS 0311	9.46	26	12.79	14	3.33

SITE ID	SEC RATE (MM/YR)	SEC # POINTS	VA RATE (MM/YR)	VA # POINTS	SS RATE (MM/YR)
CRMS 0318	8.90	26	14.34	9	5.44
CRMS 0322	6.34	26	7.84	14	1.50
CRMS 0326	4.44	26	5.89	14	1.45
CRMS 0332	4.15	26	9.20	11	5.04
CRMS 0335	10.56	25	14.15	13	3.59
CRMS 0336	7.20	26	5.98	12	-1.23
CRMS 0337	6.42	26	10.96	9	4.54
CRMS 0341	11.24	25	18.54	10	7.29
CRMS 0345	14.04	25	24.99	14	10.95
CRMS 0369	3.20	24	18.86	9	15.66
CRMS 0374	8.05	26	10.84	9	2.79
CRMS 0377	4.45	24	5.09	10	0.64
CRMS 0383	9.90	25	21.64	9	11.75
CRMS 0386	6.42	26	22.23	14	15.81
CRMS 0390	13.56	26	11.68	14	-1.87
CRMS 0392	8.99	24	24.70	12	15.71
CRMS 0397	6.64	26	11.18	14	4.54
CRMS 0398	7.40	25	14.52	14	7.12
CRMS 0399	6.35	26	12.67	11	6.32
CRMS 0400	7.11	26	9.51	12	2.41
CRMS 0416	5.95	26	7.77	10	1.81
CRMS 0421	15.49	26	22.38	9	6.89
CRMS 0434	5.05	26	7.27	14	2.22
CRMS 0482	6.81	23	14.02	11	7.22
CRMS 0489	17.29	26	23.79	14	6.51
CRMS 0490	4.55	25	9.92	14	5.37
CRMS 0493	4.62	24	10.77	12	6.15
CRMS 0496	4.80	23	12.22	12	7.42
CRMS 0498	2.43	25	8.46	12	6.04
CRMS 0499	6.18	25	7.47	13	1.30

SITE ID	SEC RATE (MM/YR)	SEC # POINTS	VA RATE (MM/YR)	VA # POINTS	SS RATE (MM/YR)
CRMS 0504	8.72	25	11.78	13	3.06
CRMS 0507	-2.47	23	10.25	11	12.72
CRMS 0513	6.95	26	9.20	14	2.25
CRMS 0514	3.73	26	9.84	14	6.11
CRMS 0520	4.60	25	12.26	13	7.66
CRMS 0522	0.79	25	7.38	13	6.59
CRMS 0523	4.97	24	11.51	12	6.53
CRMS 0524	3.57	23	9.36	11	5.78
CRMS 0527	7.98	24	12.84	12	4.87
CRMS 0531	6.69	23	7.48	11	0.79
CRMS 0532	6.17	25	11.79	13	5.63
CRMS 0535	3.12	23	6.55	11	3.42
CRMS 0536	5.29	23	9.43	10	4.14
CRMS 0543	7.58	26	17.64	15	10.06
CRMS 0544	7.10	26	11.35	15	4.25
CRMS 0547	4.54	20	9.09	8	4.55
CRMS 0549	7.32	26	11.60	13	4.27
CRMS 0550	3.52	24	10.02	13	6.50
CRMS 0551	-5.79	24	9.73	12	15.51
CRMS 0552	5.94	24	10.94	12	5.01
CRMS 0553	-8.22	25	5.36	13	13.58
CRMS 0554	8.54	24	9.11	12	0.58
CRMS 0557	-7.66	21	6.57	10	14.24
CRMS 0570	18.60	22	17.41	11	-1.19
CRMS 0574	5.95	24	12.46	9	6.51
CRMS 0580	3.49	23	4.50	11	1.02
CRMS 0583	3.13	24	3.33	12	0.20
CRMS 0584	-1.91	26	6.08	14	7.99
CRMS 0587	3.74	24	2.74	12	-1.00
CRMS 0588	1.85	25	4.60	13	2.75

SITE ID	SEC RATE (MM/YR)	SEC # POINTS	VA RATE (MM/YR)	VA # POINTS	SS RATE (MM/YR)
CRMS 0599	-1.15	26	13.30	13	14.45
CRMS 0604	-2.67	24	8.55	11	11.21
CRMS 0608	-6.81	26	10.40	13	17.21
CRMS 0610	-1.70	26	4.88	12	6.58
CRMS 0614	11.50	24	8.63	9	-2.86
CRMS 0615	-1.69	26	2.30	14	3.99
CRMS 0616	3.69	25	9.12	9	5.43
CRMS 0618	3.87	26	11.22	10	7.35
CRMS 0619	9.82	23	5.82	11	-4.00
CRMS 0622	-1.94	23	1.94	9	3.89
CRMS 0624	5.12	25	4.96	13	-0.16
CRMS 0630	2.36	24	16.70	6	14.34
CRMS 0642	6.66	25	2.54	11	-4.12
CRMS 0644	1.30	23	5.75	11	4.44
CRMS 0645	3.68	23	3.90	11	0.22
CRMS 0648	2.67	24	2.74	9	0.07
CRMS 0651	-3.33	25	3.70	13	7.03
CRMS 0655	2.32	24	3.86	12	1.54
CRMS 0656	4.12	24	4.87	12	0.76
CRMS 0658	3.46	23	4.55	11	1.09
CRMS 0672	5.16	26	3.97	14	-1.19
CRMS 0677	3.27	25	2.96	13	-0.31
CRMS 0685	1.35	26	3.07	11	1.72
CRMS 0687	4.95	24	6.00	9	1.05
CRMS 0978	8.07	26	17.20	14	9.14
CRMS 1024	8.91	21	12.92	9	4.01
CRMS 1069	1.73	23	11.55	11	9.82
CRMS 1738	2.26	22	3.26	10	1.00
CRMS 1743	1.54	22	3.34	10	1.80
CRMS 1838	-6.31	24	2.72	11	9.03

SITE ID	SEC RATE (MM/YR)	SEC # POINTS	VA RATE (MM/YR)	VA # POINTS	SS RATE (MM/YR)
CRMS 2156	-5.68	25	8.87	11	14.55
CRMS 2189	4.45	24	3.47	12	-0.98
CRMS 2219	5.05	21	5.16	9	0.11
CRMS 2418	-5.76	24	6.50	12	12.26
CRMS 2493	3.94	21	9.78	9	5.84
CRMS 2568	6.53	24	11.91	10	5.38
CRMS 2608	12.37	19	20.44	6	8.06
CRMS 2614	8.91	22	19.34	6	10.43
CRMS 2830	6.61	22	8.39	10	1.77
CRMS 2854	11.62	23	6.62	11	-5.00
CRMS 3054	8.69	21	11.00	9	2.31
CRMS 3136	5.27	21	13.57	9	8.30
CRMS 3565	7.69	25	12.09	13	4.41
CRMS 3617	3.63	23	17.32	7	13.69
CRMS 3626	3.38	22	11.78	10	8.40
CRMS 3641	5.39	22	9.47	10	4.08
CRMS 3650	6.05	23	11.29	11	5.24
CRMS 3664	1.88	21	6.65	9	4.77
CRMS 3680	7.66	21	14.73	9	7.06
CRMS 3784	2.37	21	4.77	9	2.39
CRMS 3800	1.78	21	8.04	7	6.26
CRMS 3913	12.23	22	16.13	10	3.90
CRMS 3985	6.57	21	8.54	9	1.97
CRMS 4014	7.19	24	10.41	12	3.22
CRMS 4045	5.46	21	8.27	9	2.81
CRMS 4094	6.35	21	11.62	9	5.26
CRMS 4103	9.58	21	6.95	9	-2.63
CRMS 4107	-4.42	20	3.37	9	7.80
CRMS 4218	8.41	22	13.89	9	5.49
CRMS 4406	4.53	23	10.25	11	5.72

SITE ID	SEC RATE (MM/YR)	SEC # POINTS	VA RATE (MM/YR)	VA # POINTS	SS RATE (MM/YR)
CRMS 4407	1.13	23	7.67	11	6.54
CRMS 4455	8.39	26	12.73	8	4.34
CRMS 4529	7.52	23	12.02	11	4.50
CRMS 4548	7.04	22	9.71	9	2.67
CRMS 4572	5.65	22	8.73	9	3.08
CRMS 4596	4.31	23	10.43	10	6.12
CRMS 4626	13.33	23	18.13	11	4.80
CRMS 4690	6.79	26	9.76	13	2.97
CRMS 4779	4.57	20	12.15	9	7.57
CRMS 4782	3.30	21	11.37	9	8.07
CRMS 4808	4.20	20	15.03	8	10.83
CRMS 4809	1.53	19	7.79	8	6.26
CRMS 4900	10.13	24	18.74	13	8.61
CRMS 4938	5.35	20	14.52	9	9.17
CRMS 5035	9.06	20	14.64	8	5.59
CRMS 5116	6.84	21	5.75	9	-1.08
CRMS 5167	5.35	21	13.25	8	7.90
CRMS 5255	7.23	21	12.10	9	4.87
CRMS 5414	5.79	21	9.46	6	3.67
CRMS 5452	11.59	9	13.48	8	1.89
CRMS 5845	5.08	21	9.07	9	3.99
CRMS 6038	11.60	21	13.35	8	1.75
CRMS 6088	2.58	21	7.27	9	4.69
CRMS 6090	9.29	21	10.44	9	1.15
CRMS 6209	4.68	21	8.39	9	3.71
CRMS 6299	8.26	22	9.89	10	1.63

Table B3. A comparison of 2017 Coastal Master Plan subsidence ranges by 2017 subsidence polygons to 2023 Coastal Master Plan subsidence ranges. Note that these polygons are not used in the 2023 Coastal Master Plan, they serve as a reference for how subsidence values have changed between master plans.

2017 COASTAL MASTER PLAN SUBSIDENCE SUB-REGIONS		2017 RATES			2023 RATES	
		RANGE (MM/YR)	LOW/MED SCENARIO (20%) (MM/YR)	HIGH SCENARIO (50%) (MM/YR)	LOWER SCENARIO (MM/YR)	HIGHER SCENARIO (MM/YR)
1	Cheniers	1-15	3.8	8	0.1 TO 10	0.1 TO 11.2
2	Atchafalaya	3-10	4.4	6.5	5.2 TO 13.8	5.2 TO 15.6
3	BA_TE Bays	6-20	8.8	13	4.8 TO 13.9	4.8 TO 16.2
4	BA_TE Marsh	2-10	3.6	6	0.8 TO 9.8	0.8 TO 11.3
5	Breton	3-10	4.4	6.5	2.2 TO 10.9	2.2 TO 14.9
6	Pontchartrain	2-5	2.6	3.5	0.4 TO 5.2	0.4 TO 6.4
7	NO_East	3-35	9.4	19	2.1 TO 4.6	2.1 TO 5.7
8	NO_LB	2-9	3.4	5.5	2 TO 4.9	2 TO 6
9	Northshore	0	0	0	0.6 TO 3.3	0.6 TO 4.5
10	Bird's Foot	15-35	19	25	5.2 TO 22	5.2 TO 24.6
11	Bayou Gauche	2-35	8.6	18.5	3.9 TO 5.5	3.9 TO 6.8
12	Golden Meadow	6-35	11.8	20.5	5.7 TO 10	5.7 TO 11.5
13	NOLA	2-35	8.6	18.5	2.5 TO 5.2	2.5 TO 6.5
14	Mississippi River	6-25	9.8	15.5	3.2 TO 9.8	3.2 TO 11.1
15	SW Polders	1-6	2	3.5	0.8 TO 1.5	0.8 TO 1.9
16	Salt Domes	-3- -2	-2.8	-2.5	N/A	N/A
17	NA	2-35	8.6	18.5	4.9 TO 6	4.9 TO 7.3

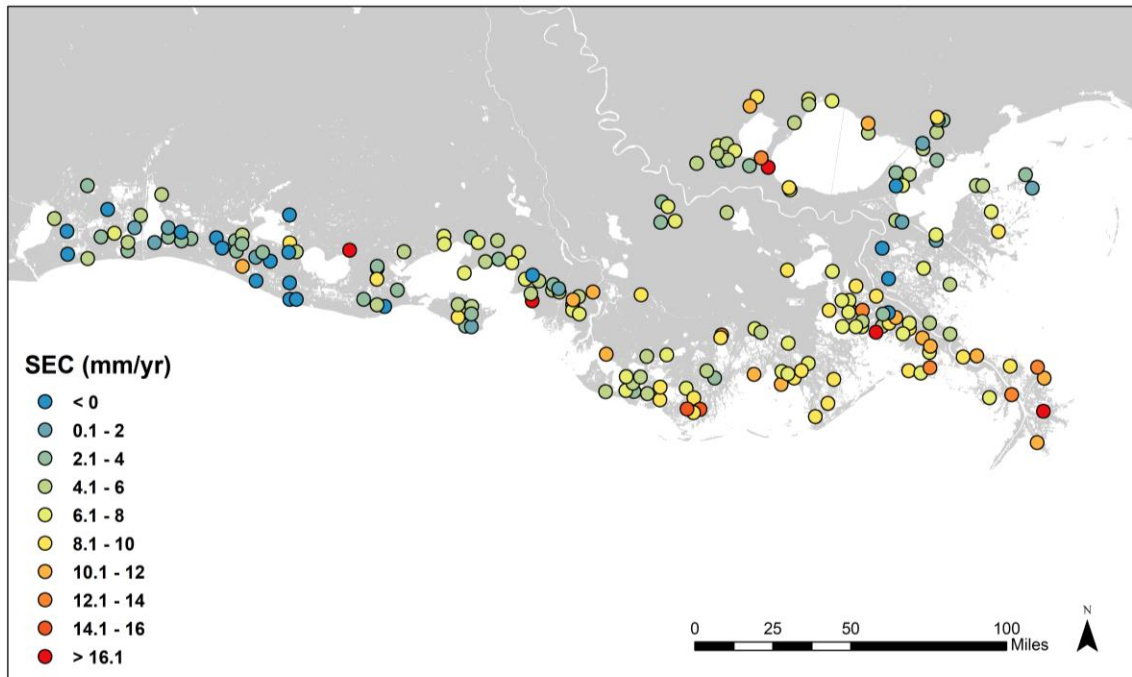


Figure B3. The distribution of surface elevation change (SEC) rates (from site establishment through fall 2019 measurement campaigns) at CRMS sites across coastal Louisiana.

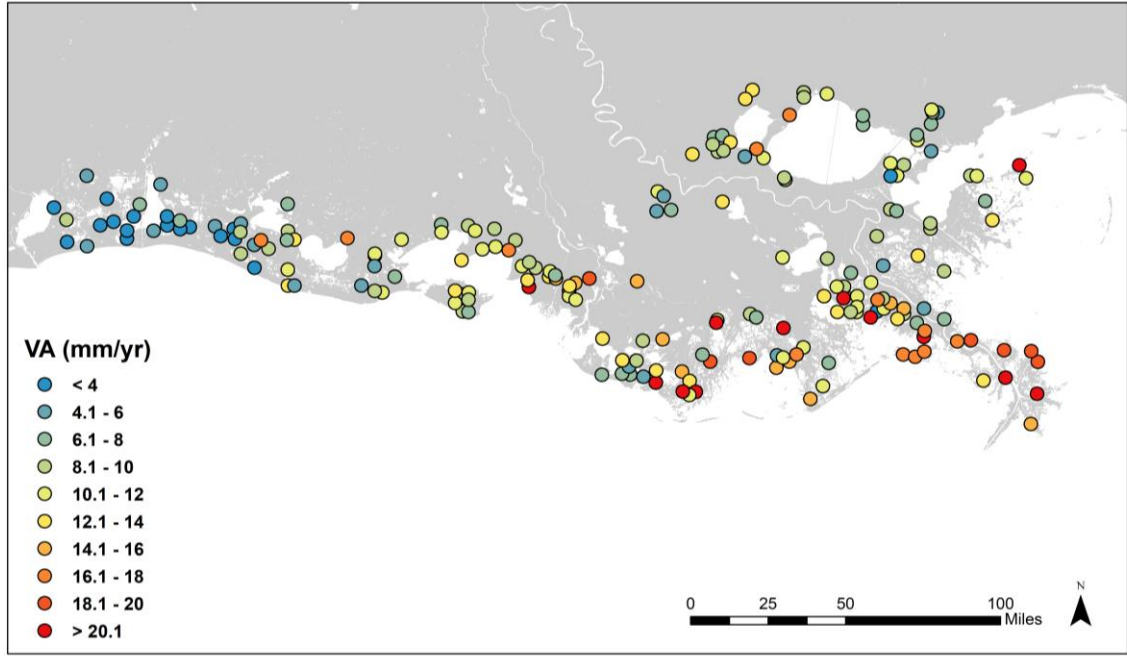


Figure B4. The distribution of vertical accretion (VA) rates (from site establishment through fall 2019 measurement campaigns) at CRMS sites across coastal Louisiana.